UNIVERSITY OF CAMBRIDGE

Department of Engineering

Plugging during rotary pile driving

Author Name: Jennifer Chambers

Supervisor: Dr Stuart Haigh

Date: 29/05/2019

I hereby declare that, except where specifically indicated, the work submitted herein is my own original work.

Signed ______________________________ *Date* ____________________

Technical abstract

The press-in method of pile driving is becoming more frequently chosen for installing piles in urban areas and confined spaces, using the negative shaft friction of previously installed piles to provide the reaction force. Thus piles can be jacked in, creating greatly reduced levels of noise and vibration. However, a major disadvantage of this is the limit it places on the available installation force, and therefore on the installed depth of the pile.

Plugging is a phenomenon which occurs in hollow tubular piles when the internal shaft friction builds up such that it is easier for the soil column inside the pile to move down at the same rate as the pile. The vertical effective stress in the soil column inside the pile increases exponentially with depth, so a pressure bulb quickly forms around the base of the pile. This is undesirable if the pile is required to resist lateral loading, since the lateral resistance of a pile depends strongly on its installed depth.

Rotary pile driving involves rotating the pile during its installation in order to reduce the required installation force. This results in the direction of the shaft friction becoming close to horizontal. The shaft friction is then resisted by the applied torque, so the applied vertical force must only resist the base resistance. The stresses in the soil column inside the pile no longer increase exponentially, so in theory, the pile should not plug when using rotary pile driving.

This project was carried out in collaboration with Giken, a Japanese company which designs, develops and operates pile-driving machines. Full-scale tests were carried out in Japan in July and August 2018 to investigate the size, shape, position and development of the pressure bulb formed during plugging. Cone penetration tests (CPTs) were used to quantify the stress states in the soil before, during and after installing piles.

The results showed that a pressure bulb roughly 2 pile diameters wide is formed as a result of plugging. Inside the pile, this pressure bulb was centred at the pile base, whereas outside the pile, it was centred slightly above the pile base.

The internal soil was found to start rotating with the pile after about 0.5 pile diameters of installation, at which point the resistance against plugging that rotary pile driving provides is lost. Model tests were subsequently carried out to investigate a hypothesis formed from these results: that preventing the rotation of the internal soil delays the onset of plugging.

The method used to prevent the rotation of the internal soil used a thin pile installed before the tubular pile, along the same centreline. The thin pile had to be installed deeper than the tubular pile so that it was well anchored and would not rotate. Two different cross-sections of pile were used to compare their effectiveness at preventing the rotation of the soil.

This method was found to be effective at preventing the rotation of the internal soil. However, this did not produce a corresponding increase in the achievable installed pile depth for a given installation force, because the prevention of rotation led to a quickly increasing torque. This meant that the limit on the available torque was reached before the limit on force, at which point, the pile could not be installed any further.

This method of preventing the rotation of the internal soil could be used in future if a wider range of pile cross-sections is investigated to find the optimum shape, or if the torque capacity of the pile-driving machine is increased. A lower bound analysis was carried out, which showed that the torque that could be provided by three reaction piles was significantly higher than the current torque capacity of the pile-driving machine.

Contents

1 Introduction

1.1 Background

Hollow cylindrical steel piles of any diameter can be manufactured by helically welding sheets of steel into tubes. The use of the 'gyropiling' method to install this type of pile is becoming more popular, pioneered by Giken Ltd with their rotary pile-driving machines (see *figure 1*). Tubular piles are commonly used for retaining walls, watertight cofferdams and disaster prevention levees. In 2018, Giken completed construction of an 'Eco Park' underground parking structure in the city centre of Kochi, Japan (GIKEN Ltd, 2018). The structure consists of 55 tubular piles installed to create an earthquake-proof underground car park with a capacity for 60 cars, but with a minimum above-ground footprint.

Figure 1: Giken gyropiler (photo: JE Chambers, 2018).

As a tubular pile is installed, it may enter the soil in either an unplugged or a plugged manner. Initially, the pile cuts into the soil leaving the internal soil stationary, entering in an unplugged manner (also referred to as coring). As the pile is installed further, the internal shaft friction increases and eventually becomes larger than the resultant of the base resistance and the weight of the plug, shown in *figure 2*. Beyond this point it is easier for the pile to enter the soil in a plugged manner, with the internal soil moving down at the same rate as the pile.

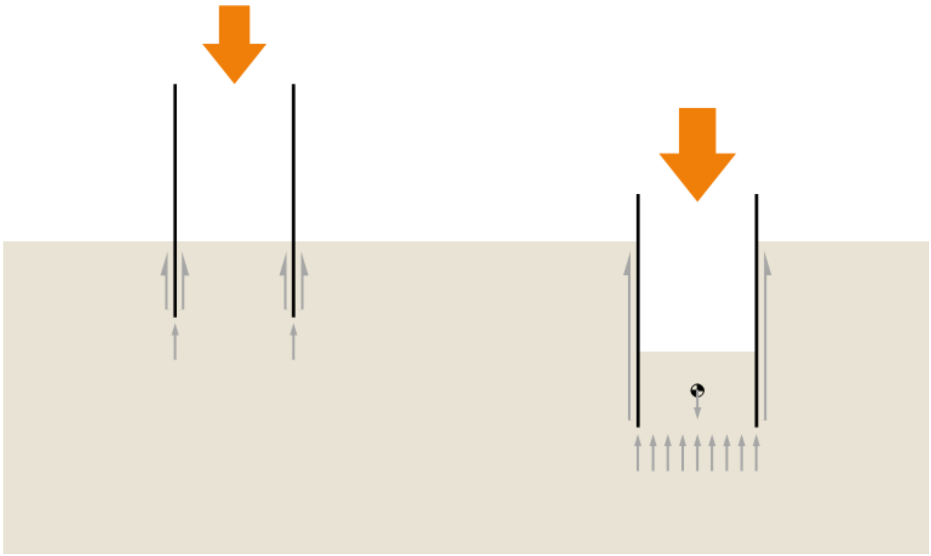

Figure 2: Forces acting on unplugged (left) and plugged (right) piles.

It can be shown that the vertical stress in the soil plug increases exponentially with depth, which makes it difficult to install the pile further once it has started to plug. This may be desirable if the piles are only required to resist vertical loads, since the build-up of stress leads to a large base capacity at a shallower depth. However, the resistance to horizontal loads depends heavily on the length of the pile, so plugging is unwanted when horizontal loads are expected because it slows the installation rate, and may prevent further installation altogether.

Rotary pile driving involves slowly rotating the pile as it is pushed downwards into the soil. The main benefits of this method are that it should theoretically prevent plugging from happening, and that the installation force is reduced since the shaft friction component is now resisted by the torque.

1.2 Giken–Cambridge collaboration

This research was carried out in collaboration with Giken, a Japanese company which designs, develops and operates pile-driving machines. Their range of Silent Piler machines install piles using the press-in method, which involves jacking piles into the soil with hydraulic rams, exploiting the negative shaft friction of previously installed piles to provide the necessary reaction force. The press-in method creates considerably less noise and vibration than traditional vibratory or hammering pile-driving methods, so it is ideal for construction work in urban areas or near sensitive buildings. However, the achievable installation depth is limited by the maximum reaction force that can be provided by the reaction piles.

The experiments described in section 3 were carried out in Kochi, Japan in July and August 2018, by two students from the University of Cambridge and a team of engineers from Giken. Improved knowledge and understanding of soil behaviour during pile installation will enable Giken to achieve faster installation to the desired depth in all types of soil. This research involves full-scale tests using the press-in method, whereas almost all previous research into plugging has either been model testing or only considering driven piles.

2 Literature Review

2.1 The press-in method

The main advantages of the press-in method are the significantly reduced levels of vibration and noise compared with driven piles, and the ability to carry out piling work in a confined space (White et al, 2000).

The level of vibration and noise caused by the press-in method was investigated by Rockhill et al (2003) by analysing recordings of vibrations at test sites and construction sites. Transient vibrations caused by the release of elastic stresses in the pile when the chuck is opened and closed are of a much larger magnitude than the continuous ground vibrations due to the generator and crane. The separation between piling operations and sensitive structures can be reduced by a factor of 10–50, and between piling operations and the public by a factor of up to 5, compared with those required when using traditional pile-driving methods.

The nature of the press-in method means that it can be adapted for carrying out piling work on sites with limited clearance. Giken has developed dedicated piling machines for piling with limited clearance overhead or to adjacent structures (GIKEN Ltd, n.d.).

When using a traditional pile-driving method, the applied driving forces cause very high stresses in the pile. These high stresses are not present when using the press-in method since the applied forces are much lower, so pile damage due to high driving stresses is avoided (Finlay et al, 2001).

However, a considerable disadvantage of the press-in method is the limit on the installation depth imposed by the available reaction force from the reaction piles. An increase in resistance from the soil beyond the reaction force available will prevent further installation by the press-in method. With traditional pile-driving methods, an increase in resistance from the soil may result in a reduced installation rate, but is unlikely to prevent any further installation (Finlay et al, 2001).

Finlay et al (2001) also presents various techniques to improve the maximum installation rate and depth that can be achieved with the press-in method:

i. surging, discussed in section 2.2 below
ii. water jetting, which involves injecting large volumes of water into the soil through a pipe attached to the pile base
iii. driving shoes, which reduce the internal shaft friction due to a modified flow of soil into the pile
iv. pre-augering, which weakens the ground before pile installation.

2.2 Surging

Surging involves cyclically moving the pile up and down during installation to attempt to install the pile further without increasing the applied vertical force (Delano, 2010). The cyclic loading shears the soil in contact with the pile shaft, causing densification. This reduces the horizontal stress, and therefore the friction, acting on the pile shaft. This reduction in friction due to cyclic loading is referred to as friction fatigue. The base resistance is also reduced by surging, through particle crushing and rearrangement.

2.3 Water injection

Water injection is a technique to increase installation rates and reduce the required installation forces (Shepley and Bolton, 2014); it involves injecting water through a pipe attached to the base of the pile. The installation force is reduced through two mechanisms (Tsinker, 1988). Firstly, the natural structure of the soil immediately surrounding the nozzle is destroyed by the water jet, reducing the base resistance. The water then filters towards the ground surface along the side of the pile, lubricating the pile shaft and reducing the shaft friction.

Note that water jetting refers to much higher flow rates than water injection.

2.4 Rotary pile driving

Rotary pile driving (also referred to as 'gyropiling' or the 'gyropress method') is the method of rotating the pile while pushing it into the soil (Ishihara et al, 2015), as shown in *figure 3*. A ring with 'teeth' can be fitted onto the base of the pile to help cut through the soil as the pile is rotated.

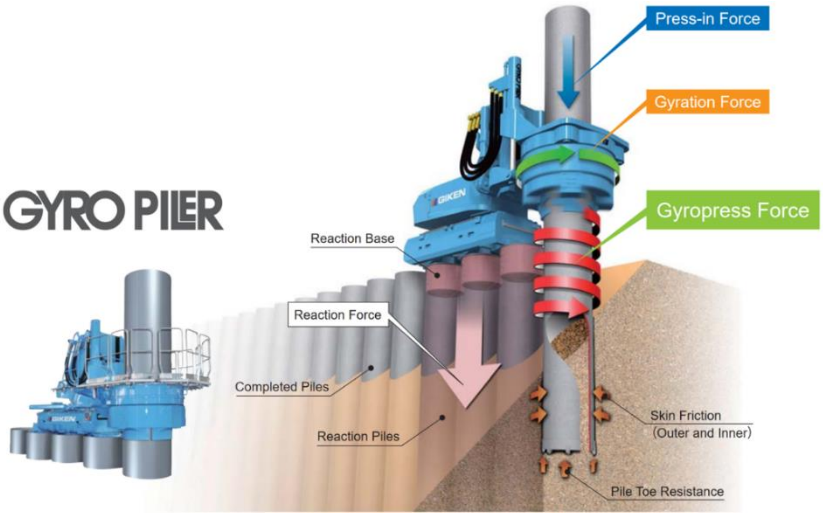

Figure 3: The gyropress method (GIKEN Ltd, 2018).

It is important to differentiate between the use of rotation to cut through obstacles in the soil, and the use of rotation as a technique to reduce installation forces, as was the case in the experiments carried out in this project. A ring with extra cutting teeth can be used such that, if the pile is rotated fast enough, it can core through reinforced concrete (GIKEN Ltd, n.d.).

2.5 Plugging

Randolph et al (1991) carried out a numerical analysis to find the stresses acting in the soil plug inside a tubular pile. They considered an element taken from the soil column inside the pile, shown in *figure 4*. Vertical equilibrium of this element results in an expression for the vertical stress at the base of a soil plug of length h (see *appendix A* for the full derivation):

$$\sigma_v' = \frac{\gamma' h}{\lambda}\left(e^{\lambda} - 1\right)$$

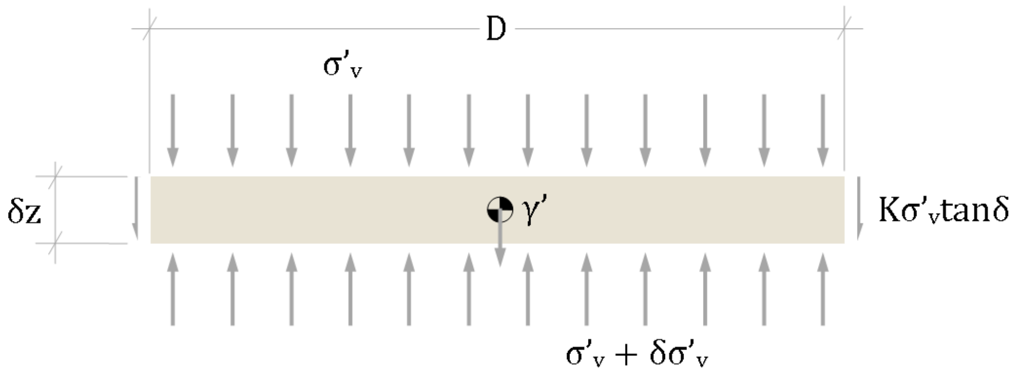

Figure 4: Equilibrium of an element from the soil column inside the pile.

Randolph et al (1991) also introduced the concept of an active length of plug. This is the lower part of the soil column inside the pile, over which the internal shaft friction is assumed to be mobilised. The upper part of the soil column is conservatively assumed to act as a surcharge. The vertical stress at the top of the active plug is therefore equal to the weight of the inactive part of the soil column. This is applied as a boundary condition when the equilibrium equation is integrated to find the vertical stress distribution through the active length of plug. However, the parameters in the exponential term must be precisely determined in order to use the resulting equation (Lehane and Gavin, 2001).

Lehane and Gavin (2001) carried out model testing to investigate the influence of the in situ stress, pile diameter and wall thickness on the base capacity of jacked piles. They found that piles which were partially plugged had a base capacity proportional to the incremental filling ratio (IFR), whereas piles which were fully plugged had a base capacity comparable to the cone penetration test (CPT) tip resistance at the base of the pile.

The IFR is a convenient measure of the degree of plugging, and can therefore be used to determine the relationship between the degree of plugging and various parameters related to pile installation. An increase in IFR corresponds to a decrease in the degree of plugging. Murthy et al (2018) found that the IFR increases with increasing pile diameter, and decreases with increasing installed depth.

Henke and Grabe (2008) carried out a numerical analysis of the influence of the installation method on the plugging behaviour. They calculated the horizontal stresses inside and outside a 0.61 m diameter pile jacked 4.5 m into medium-dense sand. Inside the pile, there is a peak in horizontal stress level with the base of the pile, which is larger in magnitude closer to the pile wall. Outside the pile, the peak is much smaller in magnitude, and is just above the base of the pile.

Henke and Grabe (2008) explained that the high horizontal stresses around jacked piles are due to the dilatancy of the soil. Around driven piles, these high stresses are not observed, so plugging is unlikely to occur.

Miller and Lutenegger (1997) carried out full-scale tests to establish the relationship between pile plugging and shaft friction. They suggested that plugging increases the shaft friction because of the horizontal stresses that develop during plugging, and identified two parameters which affect the plugging behaviour:

i. method of installation – jacked piles displayed a greater degree of plugging than driven piles
ii. pile geometry – piles with smaller diameters displayed a greater degree of plugging.

Kikuchi (2008) carried out tests on long, large-diameter piles jacked into model ground, monitoring the penetration resistance and the level of the ground surface inside the pile, H. The results showed intermittent plugging; the penetration resistance exhibited sudden dips and peaks, while H showed corresponding changes in gradient.

Kikuchi (2008) then carried out CPTs inside and outside the pile to measure the change in ground strength around the pile before and after installation. *Figures 5 and 6* show the CPT tip resistance inside an unplugged and a plugged pile, respectively. The unplugged pile shows two peaks in the stress inside the pile. The first peak was assumed to be a result of the pile wall, while the second peak was thought to be due to the stress increases caused by the pile installation. The plugged pile shows a single peak just below the base of the pile, but of a much larger magnitude than the peaks for the unplugged pile.

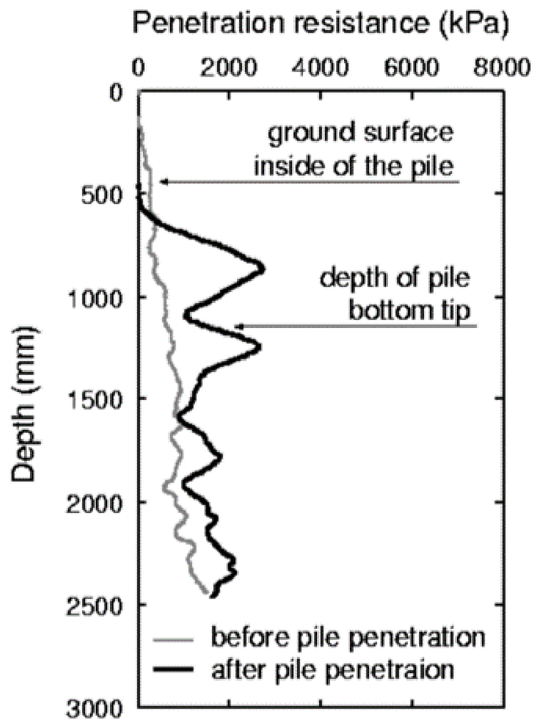

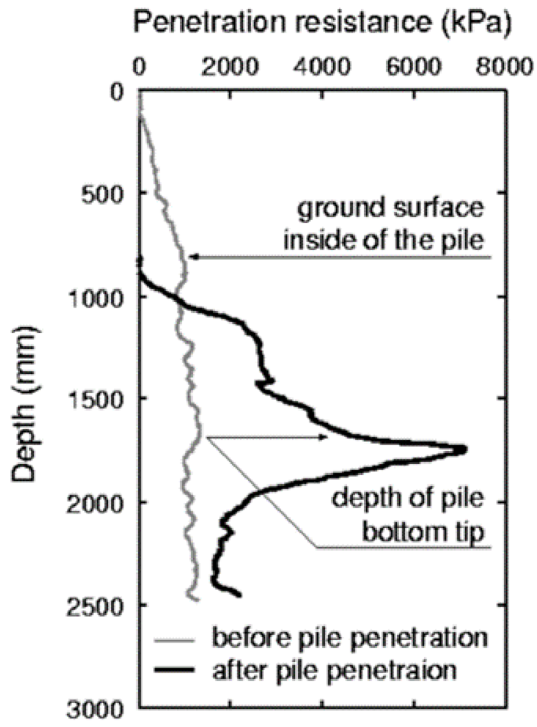

Figure 5: CPT tip resistance inside an unplugged pile (Kikuchi, 2008).

Figure 6: CPT tip resistance inside a plugged pile (Kikuchi, 2008).

CPTs were also carried out one pile diameter away from the centre of the pile (Kikuchi, 2008). The unplugged pile had no effect on the CPT tip resistance at this distance from the pile centre. However, the plugged pile caused a significant change to the CPT tip resistance outside the pile. The resistance near the soil surface decreased due to the dilatancy of the sand upon shearing. The resistance below the pile base increased because this soil was compressed by the pile installation.

The previous research that is most similar to the proposed experiments for this project is the full-scale tests on plugging in jacked piles carried out by White et al (2000). They used an instrumented pile to measure the horizontal forces in the soil, whereas the experiments in this report used CPTs to measure the stress states in the soil. The results from the instrumented pile suggest that arching theory suitably predicts the internal shaft friction. They hypothesised that pile installation using the press-in method could be improved with the use of driving shoes or water injection.

Ko and Jeong (2015) also carried out full-scale tests to investigate the effect of plugging on the pile capacity, but they used a hydraulic hammer to install the piles rather than the press-in method. They found that the internal shaft resistance was mostly mobilised by the lower part of the pile.

2.6 Cone penetration test (CPT)

CPTs can be used to estimate the lateral stresses in soils, provided the overconsolidation ratio (OCR) is known or can be estimated. Masood and Mitchell (1993) proposed an equation for calculating the effective stress friction angle from the CPT sleeve friction and the in situ vertical effective stress. The coefficient of lateral earth pressure at rest can then be estimated from the OCR and the effective stress friction angle. Using this and the in situ vertical effective stress, the in situ horizontal effective stress can be estimated.

CPTs have successfully been used in the past (Finlay et al, 2001) to quantify the in situ stresses and to compare the stresses in the soil before and after pile installation. In this report, the CPT tip resistance will be used as a way of quantifying the stress state in the soil, rather than using a correlation to calculate the actual horizontal and vertical effective stresses.

3 Primary Experiments

3.1 Theory and design of experiment

Consider the same element from the soil column inside the pile as in section 2.5, but now with rotation of the pile. If the pile is rotated fast enough compared to its vertical velocity, the resultant velocity of the pile relative to the internal soil is almost horizontal. This means that the internal shaft friction term disappears from vertical equilibrium, as shown in *figure 7*, resulting in a vertical stress distribution inside the pile that increases linearly with depth (see *appendix B* for full derivation). There is no longer an exponential build-up of vertical stress, so in theory, plugging should not occur when using rotary pile driving.

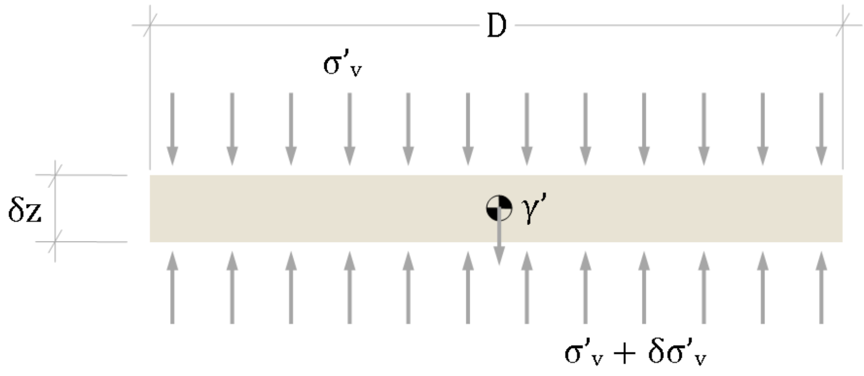

Figure 7: Equilibrium of an element from the soil column inside the pile when using rotary pile driving.

Based on the theory discussed in section 2, the CPTs were expected to give results similar to the graphs shown in *figure 8*. If the pile had plugged, it was expected that the CPT tip resistance inside the pile would have an exponential shape. Outside the pile, it was expected to peak at around the depth of the base of the pile since the installation creates a pressure bulb: a stress concentration surrounding the pile base which decreases in intensity further away from the pile base. If the pile had not plugged, it was expected that the CPT tip resistance would be similar to the in situ values.

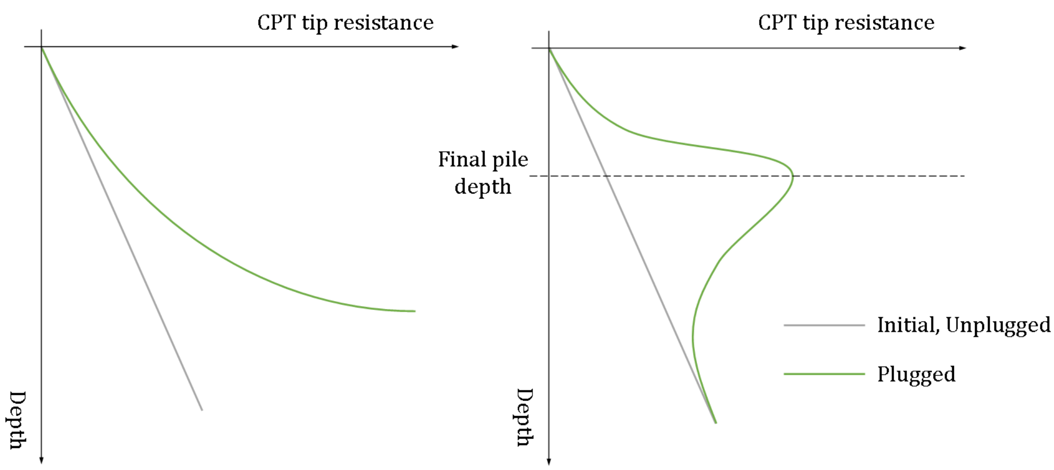

Figure 8: Expected CPT results.

The main objectives of this project were:

i. to investigate the pressure bulb distribution after pile installation
ii. to investigate the development of the pressure bulb during pile installation
iii. to propose methods for preventing plugging during rotary pile driving.

3.2 Apparatus and experimental techniques

3.2.1 Test site

The tests described in section 3 were all carried out at the Niida test site in Kochi, Japan. It is a coastal river outwash plain, and was investigated in 1995 with three boreholes (Carter, 1996). The results of the standard penetration tests (SPTs) showed that the site consists of medium-dense to dense sand for the first 4–5 m, and sandy gravel below that. The water table lies 7.25 m below the ground surface, which is well below the installation depth of the piles in these tests, so effective and total stresses are equal.

3.2.2 Experiment cases

Three different types of experiment were planned to investigate the pressure bulb distribution and development:

Case 1: The pile was installed, then CPTs were carried out at various distances from the centre of the pile. CPTs were carried out both inside and outside the pile in order to measure the change in pressure bulb distribution due to the installation of the pile.

Case 2: Similar to case 1, except a 400 kN load was applied to the pile head while the CPTs were carried out. These tests were expected to confirm the same shape and position of pressure bulb as for the case 1 tests, but with a slightly larger magnitude.

Case 3: The CPT rod was attached through the centre of the pile and both were installed simultaneously so that the development of the pressure bulb could be recorded. The CPT rod tip was attached at various distances above the pile base in order to monitor the change in stress with time.

3.2.3 Equipment

There were four tubular piles of slightly different sizes used in the tests, as shown in *table 1*. All piles also had a ring attached to their base of diameter 1010 mm, thickness 22 mm, and length 50 mm, with four cutting teeth.

Table 1: Pile dimensions.

Pile	Pile diameter (mm)	Pile thickness (mm)	Pile length (m)
A	1000	9	2.53
B	1000	12	4.12
C	1000	12	6.31
D	1000	12	9.98

A Giken F401-G1200 Silent Piler was used to install the piles for these experiments. This piling machine is compatible with piles between 0.8 and 1 m in diameter; for these experiments, 1 m diameter piles were used. It was not practical to use reaction piles to provide the reaction force, because it is likely that the proximity of the reaction piles to the test pile would have affected the results. Instead, four 130 kN weights were placed on the sides of the piling machine to provide a maximum installation force of 600 kN and a maximum torque of 300 kNm. This value of force arises from the combined weight of the piling machine and the four weights, but reduced by a safety factor to prevent unsafe movement of the piling machine.

The piling machine recorded the elapsed time, depth of the pile base, and applied force and torque every 0.1 s throughout the installation and extraction of each pile.

A laser distance-measurement device was used to measure the plugging depth of the piles by recording the inner soil depth (ISD), as defined in *figure 9*. From these measurements, the inner soil length (ISL) was calculated; this is used throughout the analysis in this report as a measure of the extent of plugging. An ISL equal to the pile depth (PD) means that the pile is coring, while an ISL less than the PD indicates plugging. The IFR can be defined using these distances:

$$IFR = \frac{\Delta ISL}{\Delta PD}$$

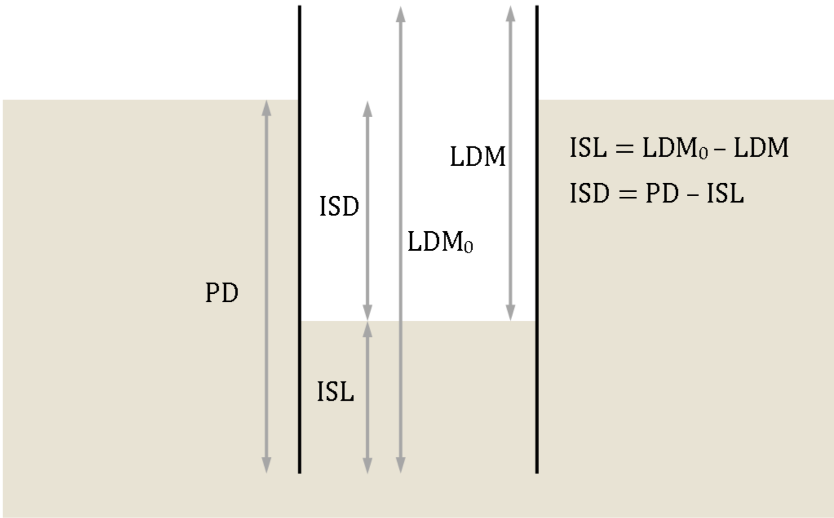

Figure 9: Relationship between ISL, ISD and PD.

The CPT rod measured the tip resistance, sleeve friction and pore water pressure every 1 cm throughout its installation. The CPT rod had a diameter of 36 mm, and consisted of several 1 m sections which were connected on and jacked into the soil one by one during the CPT.

The final measurement taken was the time elapsed when the internal soil first started to rotate with the pile. This was recorded using a camera attached to the top of the piling machine. The footage was used to determine the time between the piling machine starting to rotate and the internal soil starting to rotate. The time elapsed from the start of the pile installation could then be calculated using the torque measurements recorded by the piling machine to adjust for the delay between the piling machine first starting to rotate and the start of the pile installation.

3.2.4 Experimental accuracy

The major problems that were encountered in these experiments were the variable weather conditions and soil anisotropy. The main concern from the variable weather was the effect of heavy rain on the in situ effective stresses. The weather was therefore recorded so that it could be considered as a possible cause in the event of unexpected results. Soil anisotropy introduces two problems; difficulty in repeating tests and in obtaining representative measures of the initial soil conditions. Repeating tests becomes difficult because random unknown differences in soil conditions mean that an intended repeat may give very different results to the original test. It is not possible to use CPTs to find the initial stress distributions in the exact positions of the planned tests, because this would disturb the soil and affect the results of any following tests.

The laser distance measurement device only measured to a single point on the soil surface, but that surface was often not level. To attempt to confirm the automatic measurements, they were frequently checked manually using a tape measure.

3.3 Results and discussion

3.3.1 Table of tests

Table 2: Summary of results of pile installations.

Case	PD (m)	ISD (m)	Comments
1-1	2.95	0.34	
1-2	3.05	0.50	
1-3	1.97	-0.08	
1-4	2.81	0.24	
1-5	2.11	-0.08	no rotation
1-6	5.68	1.14	water injection, flow rate 30–40 l min^{-1}
1-7	3.20	0.19	ground very wet after typhoon
1-8	3.32	0.43	
1-9	3.28	0.53	
1-10	5.87	0.72	water injection, flow rate 40 l min^{-1}
2-1	2.13	-0.05	applied force 400 kN
2-2	3.20	0.36	applied force 400 kN
3-1	3.47	1.06	CPT tip 0.5 m above pile base
3-2	2.84	0.46	CPT tip 0.5 m above pile base
3-3	3.10	0.58	CPT tip 1.5 m above pile base
3-4	3.04	0.61	CPT tip 0.05 m above pile base

3.3.2 Table of CPTs

Table 3: Separate CPTs carried out.

File name	Comments
180702_No1	before any piles were installed
180702_No2	before any piles were installed
180717_No3	250 mm away from 180717_No4
180717_No4	250 mm away from 180717_No3

Table 4 summarises all of the CPTs carried out for each pile. The CPTs for cases 1-1, 2-1 and 2-2 were carried out after the pile had been extracted.

Table 4: Summary of results of CPTs.

Case	Distance of CPT from centre of pile (m)	File name
1-1	0.00	180703_No1
	1.50	180704_No1
1-2	0.00	180705_No1
	1.00	180706_No1
	1.50	180706_No2
	2.00	180706_No3
1-3	0.00	180710_No1
	0.25	180711_No1
	0.75	180711_No2
	0.75	180711_No4
	1.00	180711_No3
1-4	0.00	180712_No1
	0.35	180713_No1
	0.75	180712_No2
	0.75	180713_No2
	1.00	180713_No3
	1.00	180717_No1
	1.50	180717_No2
1-5	0.00	180718_No1
	0.35	180718_No2
	0.65	180719_No1
	0.75	180718_No3
	1.00	180719_No2
	1.50	180719_No3
1-6	0.00	180726_No1
	0.35	180726_No2
	0.65	180726_No3
	0.65	180726_No5
	1.00	180726_No4

Case	Distance of CPT from centre of pile (m)	File name
1-7	0.00	180727_No1
	0.35	180727_No2
	0.65	180730_No1
	1.00	180730_No2
1-8	0.00	180731_No1
	0.35	180731_No2
	0.67	180731_No3
	1.00	180731_No4
1-9	0.00	180809_No2
	0.35	180809_No1
	0.35	180809_No3
	0.62	180809_No4
	1.00	180810_No1
1-10	0.00	180824_No1
	0.35	180824_No2
	0.65	180824_No3
	1.00	180824_No4
	1.50	180824_No5
2-1	0.00	180720_No1
	1.50	180723_No1
2-2	0.00	180808_No1
	1.50	180808_No2
3-1	0.00	180802_No1
3-2	0.00	180806_No1
3-3	0.00	180807_No1
3-4	0.00	180829_No1

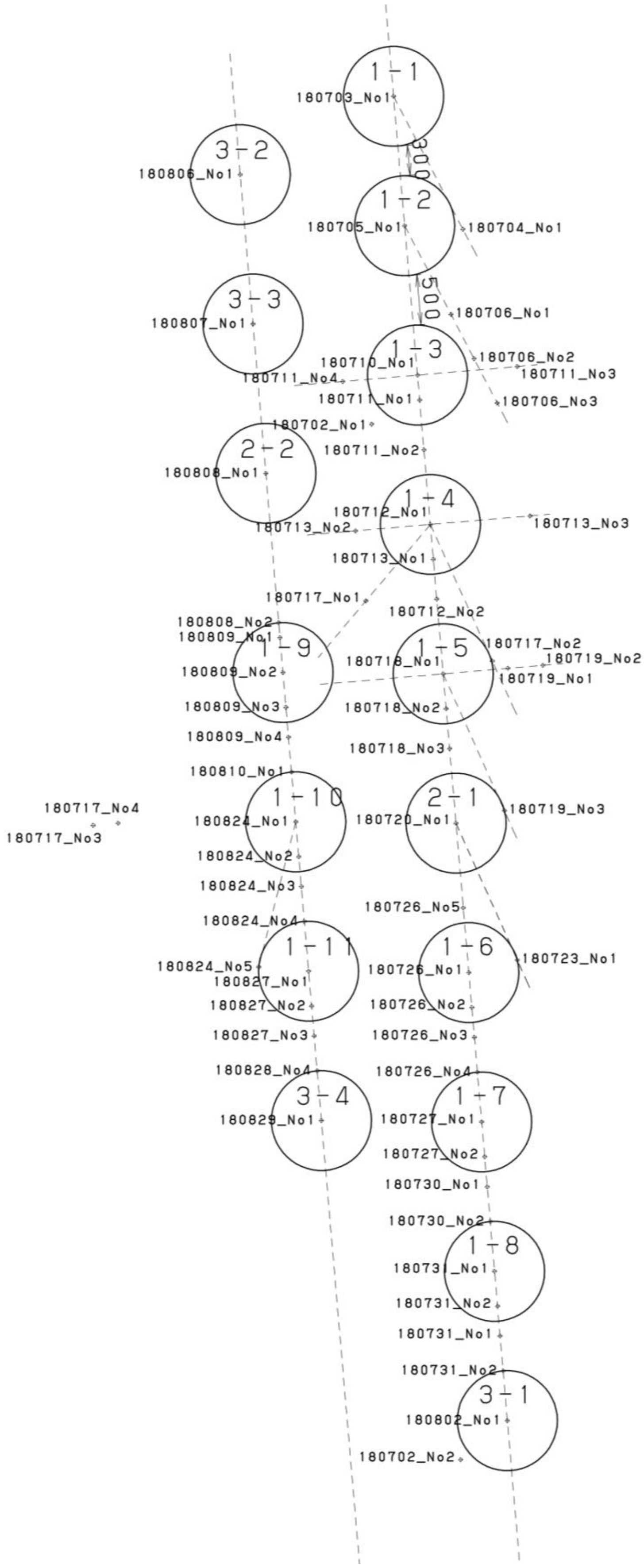

Figure 10: Positions of all CPTs (Giken, 2018).

Two CPTs were carried out far away from all other tests, and 250 mm away from each other, to investigate the extent to which one CPT affects the results of a second CPT carried out close by. *Figure 11* shows that the second CPT (shown in blue) recorded lower tip resistances, by an average of 18 per cent over the centre section. Although the first CPT compacts the soil, which would increase the tip resistance, it then leaves behind a cavity in the soil after it is extracted. When the second CPT is installed near this cavity, the soil can expand into it, providing less resistance to the CPT rod and resulting in a lower tip resistance being measured. This effect has been considered as a possible cause when CPT results were lower than expected in the analysis of the results.

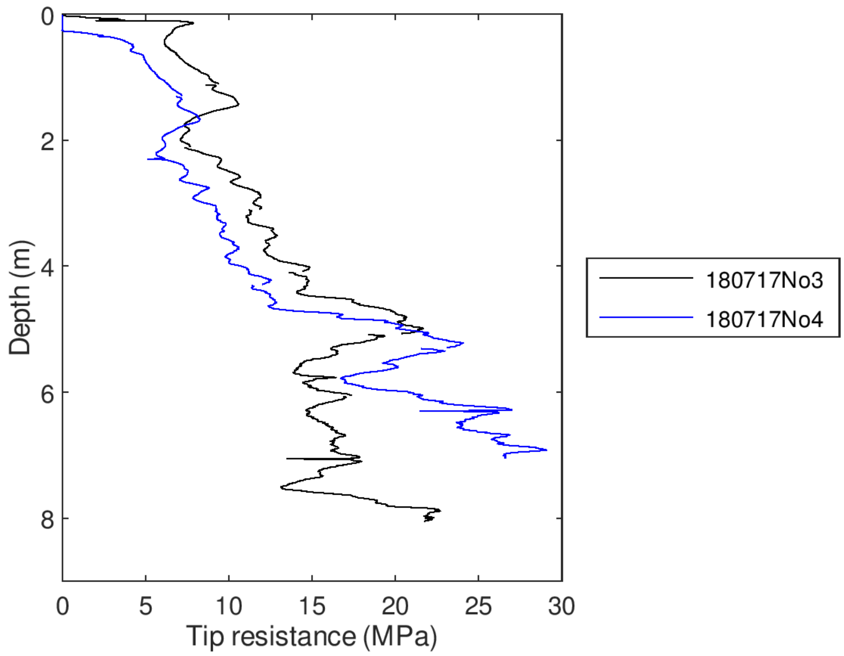

Figure 11: CPT tip resistance for two CPTs carried out 250 mm apart.

The effect of surcharge due to the weight of the piling machine was calculated to determine whether it would significantly affect the CPT results. The black line in *figure 12* is a typical distribution of initial CPT tip resistance, calculated by averaging the five 'initial' CPTs. The blue line is the stress predicted by the Boussinesq solution due to an applied surcharge. From *figure 12*, it can be seen that there is less than a 10 per cent increase in CPT tip resistance due to surcharge effects below a depth of 2.2 m.

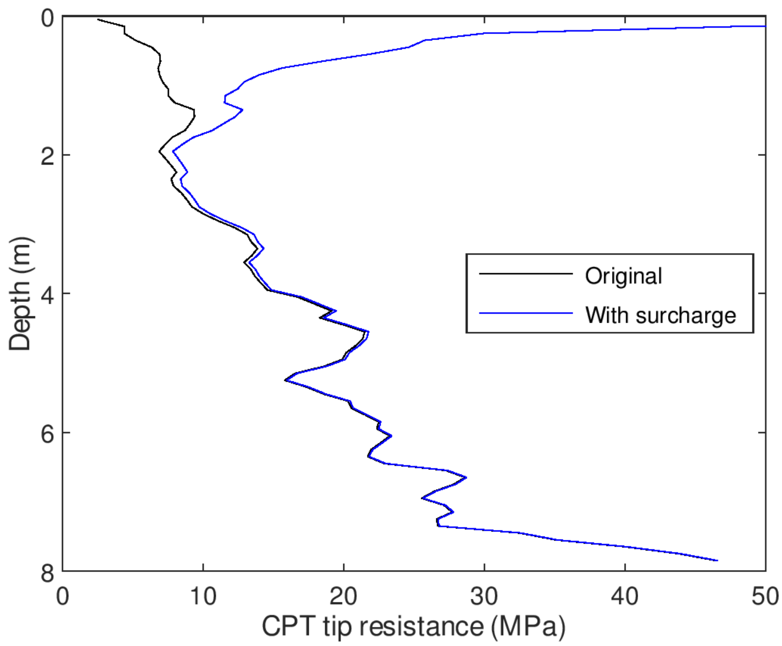

Figure 12: Effect of surcharge.

The weight of the piling machine, weights and metal sheets was assumed to be applied through a circular foundation of diameter 1.5 m, because the piling machine was placed on metal sheets of width 1.5 m. The stress applied through this assumed foundation size was calculated to be about 30 kPa, taking into account the weight of the piling machine, four weights and metal sheets.

For case 1-5, some of the CPTs were carried out directly underneath the metal plates whereas others were carried out to the side of the metal plates. If the surcharge were affecting the results, they should be different near the ground surface, but they all appear very similar over this region. Surcharge effects were therefore concluded to be insignificant and were not included in any further analysis.

3.3.3 In situ stresses

Five CPTs have been selected to represent the initial stresses in the soil. Two of these tests were carried out before the rest of the experiments started and were intended to characterise the initial stress distributions. Three further tests have been selected to give a broader initial range: the two CPTs described in section 3.3.2, which were carried out 250 mm apart, were determined to have had a small enough effect on each other that they could be considered to be representative of the initial stresses in the soil. The

CPT which was carried out 2 m away from the centre of the pile installed in case 1-2 was considered to be far enough away from the pile that it had had negligible effect on the CPT measurements.

The tip resistance distributions of these five 'initial' CPTs are shown in *figure 13*. The shaded area was calculated based on the minimum and maximum values of these 'initial' CPTs, and represents the range of likely values of initial stress with depth. It was used to determine where the most significant changes had occurred.

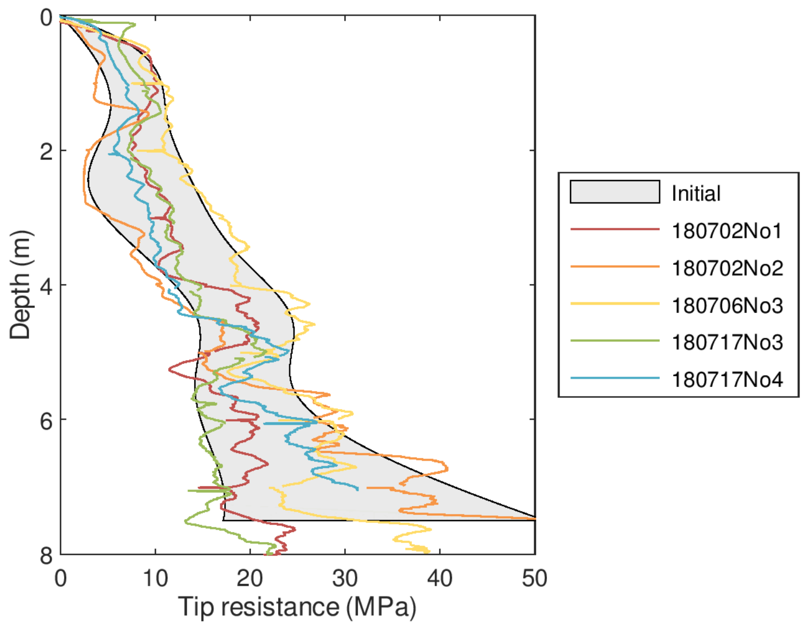

Figure 13: Initial CPT tip resistance distributions.

3.3.4 Pressure bulb

Figure 14 shows the CPT tip resistance for each of the CPTs carried out around the pile installed in case 1-4. This case has been chosen as it is representative of the trend found in the rest of the results. Note that the diameter of the pile was 1 m, so CPTs carried out less than 0.5 m away from the centre were inside the pile, and those more than 0.5 m away were outside it.

Figure 14 shows that the stress inside the pile is reduced for the top 1.5 m rather than increasing exponentially from the initial values, as might be expected. This confirms the results found by Kikuchi (2008), who suggested that it was due to the dilatancy of the sand upon shearing.

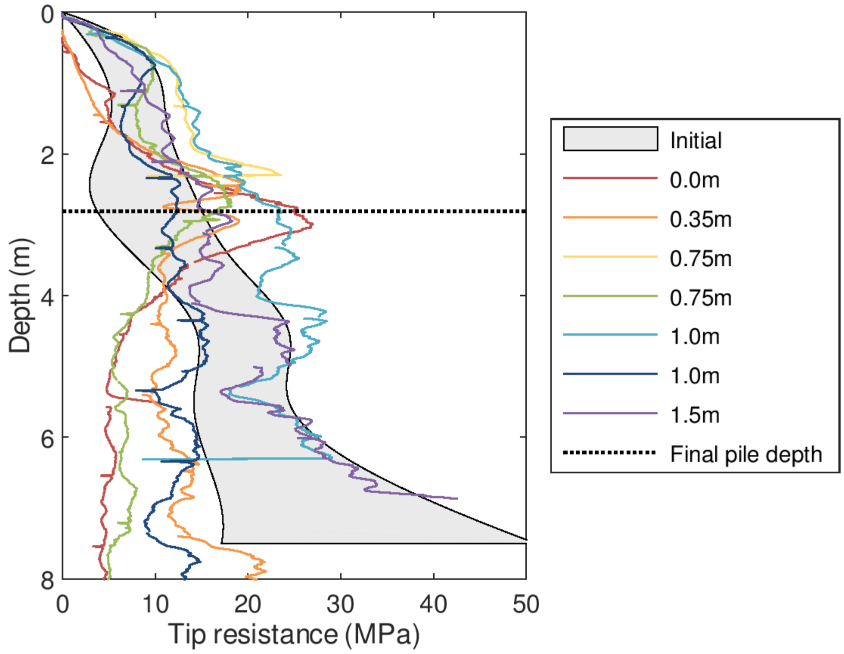

Figure 14: CPT results for case 1-4.

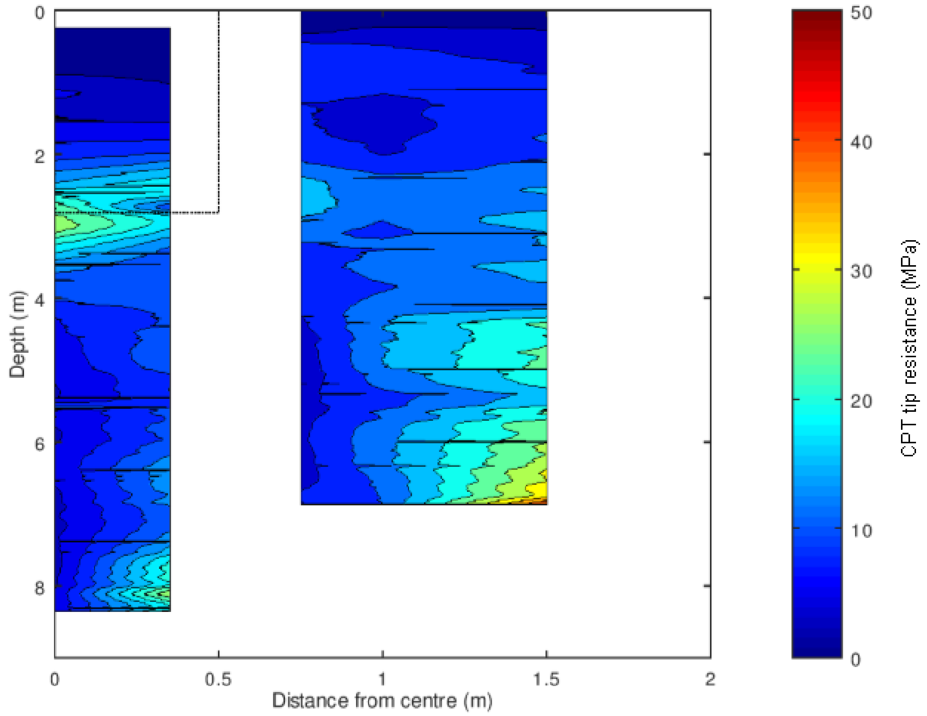

Figure 15: Contour plot of the CPT tip resistance surrounding the pile in case 1-4. Note that the black dotted line shows the final position of the pile.

Except near the pile base, soil outside the pile is not affected by the installation of the pile. This confirms the numerical analysis carried out by Henke and Grabe (2008) which was discussed in section 2.5. Level with the base of the pile, the installation has created a pressure bulb which affects an area roughly 2 m in diameter (or 2 pile diameters), shown by the contour plot in *figure 15*. The is similar to the results found by Henke and Grabe (2008) which suggested a zone of influence roughly 1.8 pile diameters wide.

3.3.5 No rotation

The pile in case 1-5 was installed without rotation, to observe the differences in stresses caused with and without rotation. The installation was ended when the required force to install the pile any further reached the limit imposed by the weight of the pile-driving machine and four weights. The ISL measurements show that the pile had not started to plug by that point.

Figure 16 shows that, inside the pile, the stress near the surface began to increase exponentially, but there was no peak at the base of the pile, which indicates that the pile was not installed far enough to start plugging.

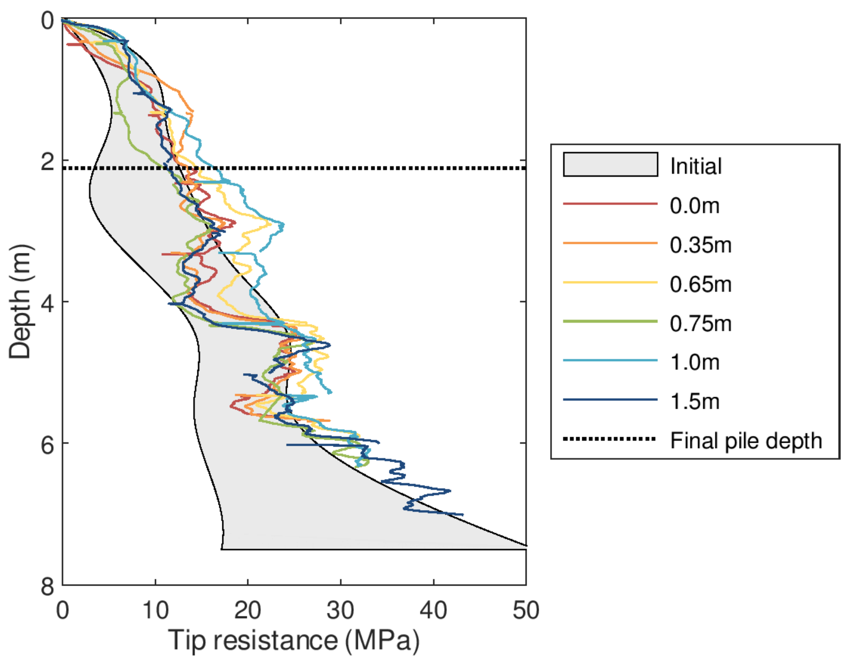

Figure 16: CPT tip resistance for case 1-5.

3.3.6 Water injection

In cases 1-6 and 1-10, water injection was used to aid the pile installation. This technique helps installation of piles in difficult soil conditions without the need to increase the applied force (see section 2.3). *Figure 17* shows the CPT results for case 1-10; the results for case 1-6 were similar but did not cover as much depth. The CPT tip resistance shows that, inside the pile, the stress is very low and not exponential in profile. Towards the base of the pile, the stress suddenly increases to match that outside the pile. Unfortunately, the CPTs were all stopped shortly below the base of the pile because the limit on the CPT rod installation force was reached at that point.

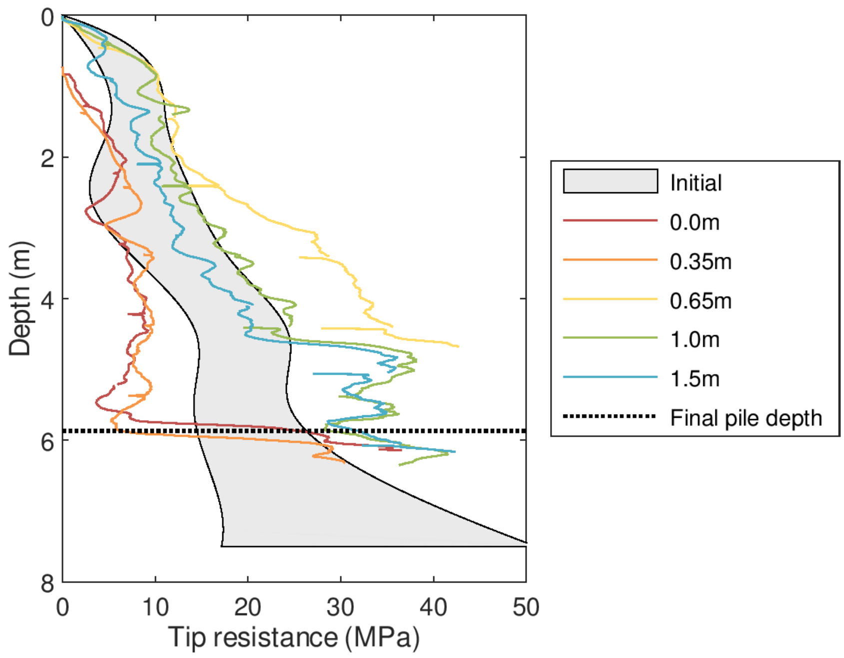

Figure 17: CPT tip resistance for case 1-10.

Outside the pile, the stress appears to increase to a peak just above the level of the base of the pile. The depth of this peak roughly corresponds to the depth of the base of the pile when plugging started. Once plugging started, the internal soil moved downwards with the pile base while the soil outside remained stationary, which explains the difference in position of the peaks in the stress distributions in the soil inside and outside of the pile.

3.3.7 Double peaks

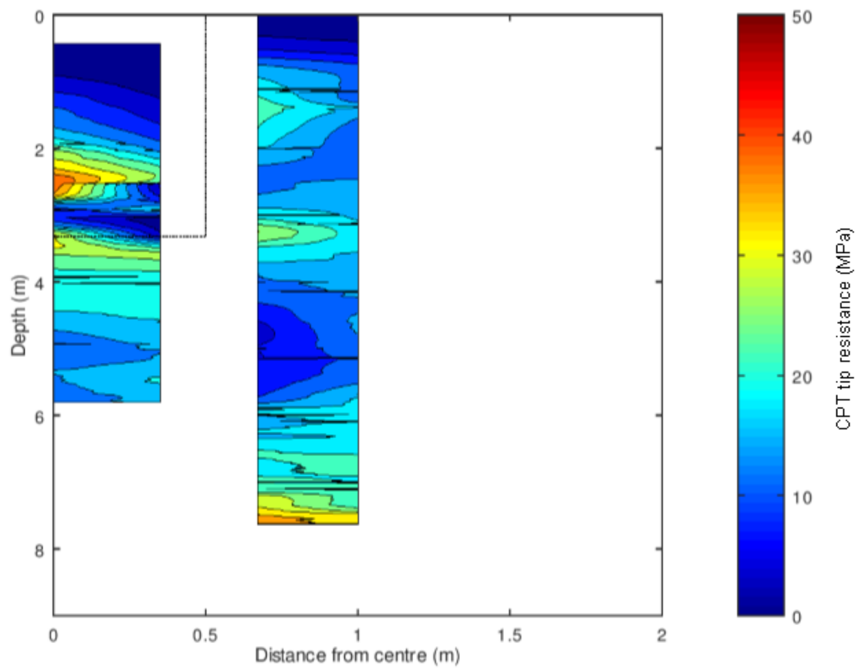

Figure 18: Contour plot of the CPT tip resistance surrounding the pile in case 1-8. Note that the black dotted line shows the final position of the pile.

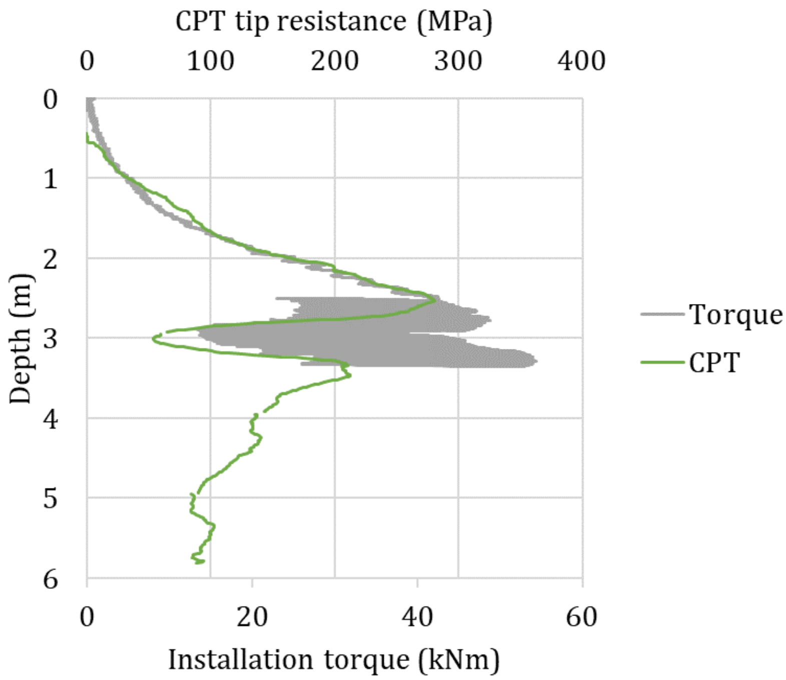

Figure 19: Installation torque and centre CPT tip resistance for case 1-8.

Figure 18 shows that there are two clear peaks in the stress measured inside the pile for case 1-8. A similar pattern can also be seen in the torque recorded by the piling machine during installation, shown in *figure 19*. This indicates two separate plugging events.

The scale over which this occurs is much larger than that for the intermittent plugging observed by Kikuchi (2008), discussed in section 2.5, so it is more likely that these double peaks are a result of a weak layer in the soil than the cyclic plugging phenomenon. When the pile base reached this weak layer, it was no longer easier for it to penetrate the soil in a plugged manner, so it progressed in an unplugged manner through the weak layer. Once it reached the end of the weak layer, it reverted back to plugged penetration.

3.3.8 Low CPT results

Some of the CPT results showed unexpectedly low stresses below depths of about 5 m; an example is case 1-4 which is shown in *figure 14* on page 22. *Figure 20* shows that the affected CPTs appear to be arranged in a cluster, so it is likely that the discrepancy is due to soil conditions that were already present before the installation of the piles, rather than a systematic error with the CPT equipment.

This test site has been used previously for many other tests, so it is possible that previous testing has caused disturbance which has resulted in these very low CPT tip resistances. *Figure 21* on p.28 is a map of previous tests which have been carried out close to the tests for this project; the tests for this project are shown in red. It shows that previous testing has been carried out only a couple of pile diameters away (dark blue area), and to depths of up to 12 m. Although the tests in the light green area were further away, they involved water injection, which is likely to affect a larger area of soil than a standard pile installation. Either of these sets of tests could have disturbed the soil in the area of the tests for this project and caused the low CPT tip resistances.

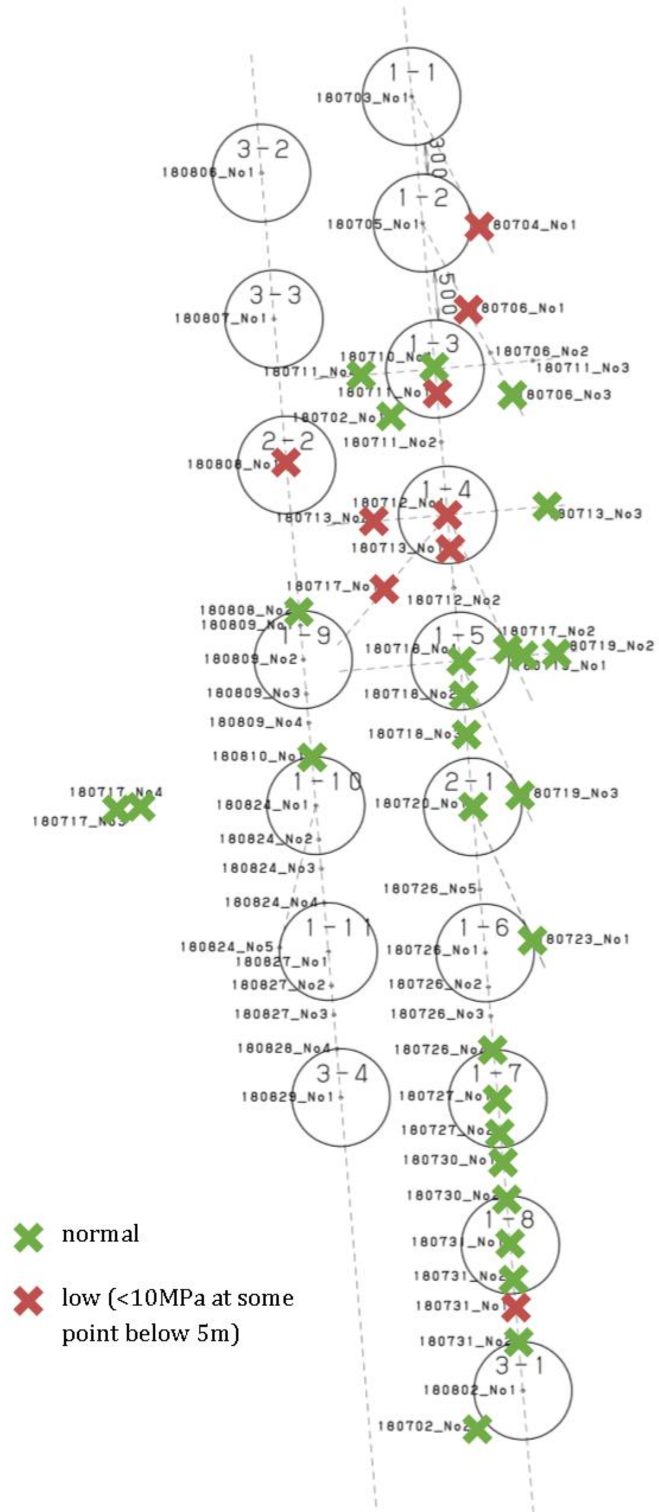

Figure 20: Layout of CPT tests highlighting ones with very low areas (Giken, 2018).

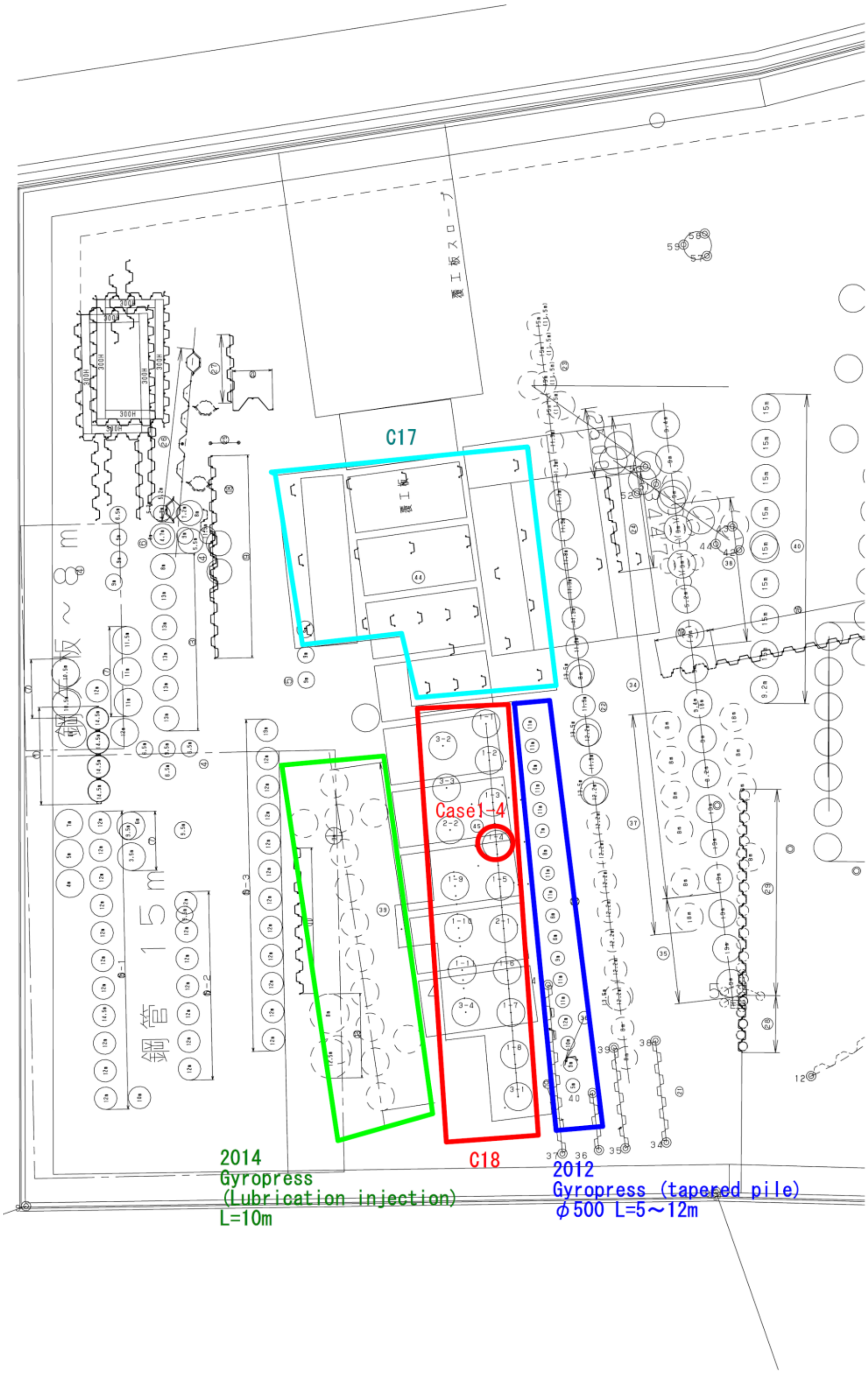

Figure 21: Map of previous testing at the Niida test site (Giken, 2018).

3.3.9 Case 2

For each of the case 2 tests, the most similar case 1 test in terms of the final installed depth and final plugging depth has been selected for comparison. Cases 1 and 2 can therefore be compared to investigate the hypothesis proposed that loading the pile during the CPT would result in a measured pressure bulb of a similar position and shape, but with a larger magnitude (see section 3.2.2).

Figures 22 and 23 show the case 2 results plotted with their corresponding case 1 tests. The results do not appear to confirm the hypothesis; instead, they seem to show that the magnitude of the pressure bulb does not increase when a load is applied to the pile.

This is most likely to be because the applied load is taken by the shaft friction rather than by the base resistance, so it has no effect on the pressure bulb around the base of the pile. The applied load is taken primarily by the shaft friction because the base response is more compliant than the shaft response. This is a result of the residual stress distribution in the pile left by the final installation stroke, which means that the shaft friction near the top of the pile acts in the opposite direction to the base capacity and the shaft friction in the rest of the pile. When a working load of 400 kN is applied (compared to the driving force of about 600 kN), the first part that mobilises is the shaft response from the top of the pile.

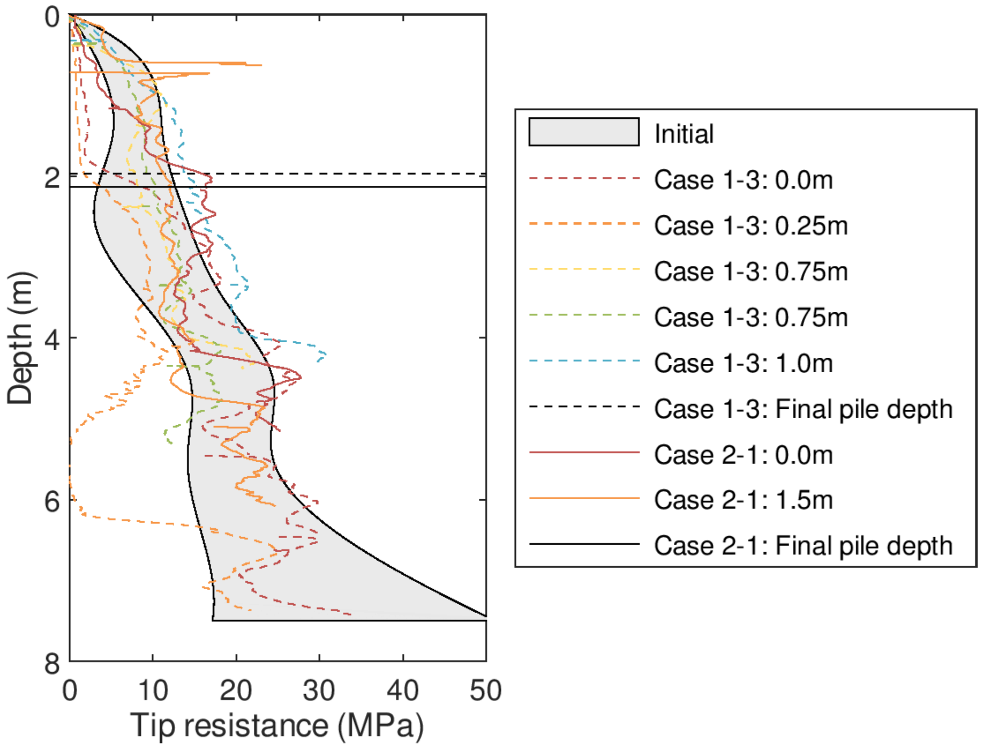

Figure 22: CPT tip resistance for cases 2-1 and 1-3.

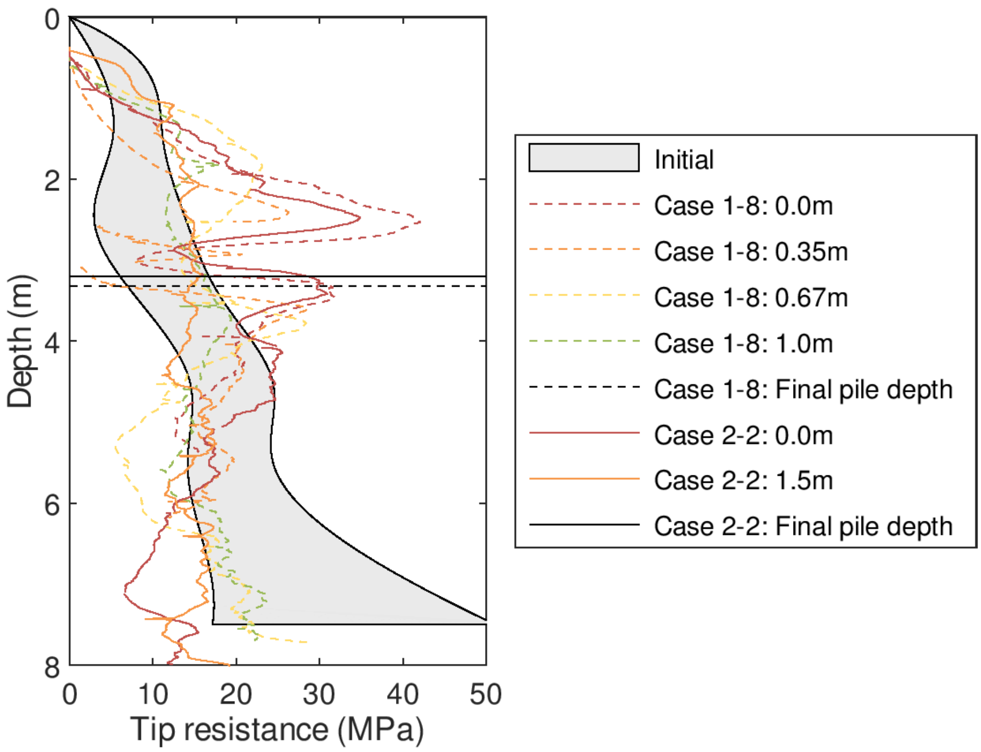

Figure 23: CPT tip resistance for cases 2-2 and 1-8.

3.3.10 Case 3

The four tests carried out for case 3 have been plotted in *figure 24*, each offset by the distance between the pile base and the CPT rod tip so that the vertical axis shows the distance of the CPT rod into the ground, rather than that of the pile. A horizontal line across the graph represents the change in stress with time in a given element of soil. Note that the results from cases 3-1 and 3-2 are very similar, indicating that the results are repeatable.

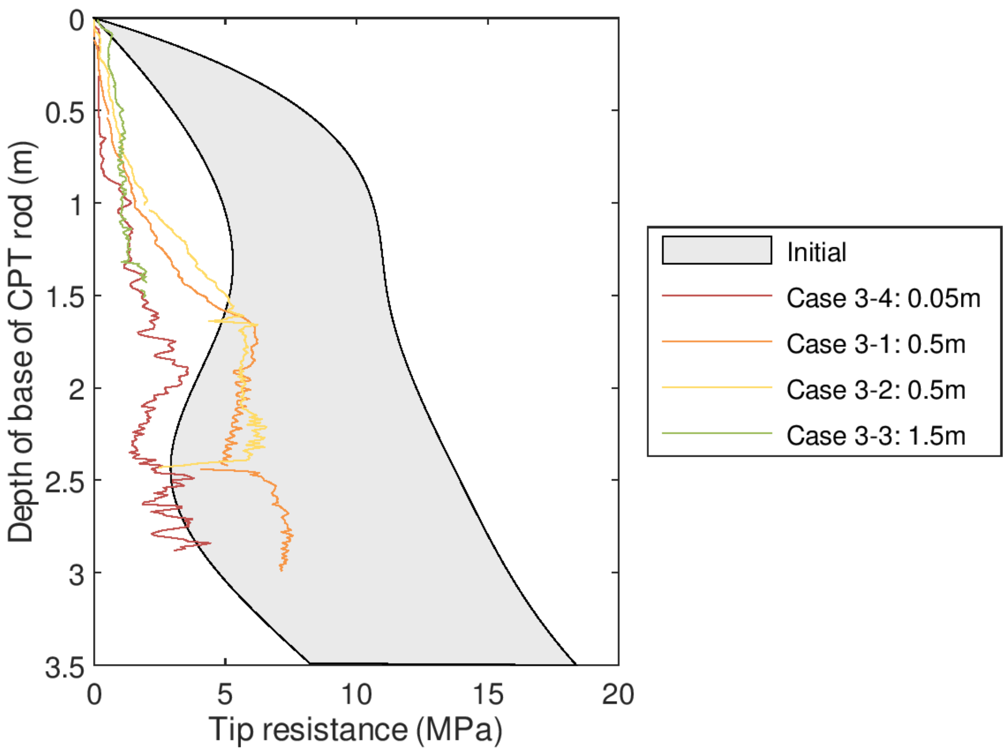

Figure 24: CPT tip resistance for the case 3 tests.

Following a horizontal line across *figure 24*, the stress in an element of soil appears to decrease from the in situ value as the pile base passes it. It has then increased by the time the pile base has been installed another 0.5 m, but decreases again as the pile installed further.

The results from case 3-4 (CPT tip 0.05 m above the pile base) are lower than expected; simple theory suggests that the stress in an element of soil at a given position should simply increase and then decrease again as the pile pushes past it. This result could be due to an error in the equipment, in which case it is incorrect and should be disregarded.

This is not unlikely since there is only one result for this test. Alternatively, it could have been correctly measured and there is a more complex mechanism affecting the soil as the pile is installed. Two possibilities will be proposed to attempt to explain this result, but it is important to note that there is a possibility that the result was incorrect, as there was no repeat due to the time-consuming nature of these tests.

The first explanation is that the four teeth on the base of the pile cut through the soil, degrading the horizontal stress. It then builds up again before the pile has penetrated a further 0.5 m.

A second explanation involves a failure mechanism such as the one shown in *figure 25*, composed of a set of wedges which do not reach the centre of the pile until about 1 radius above the pile base.

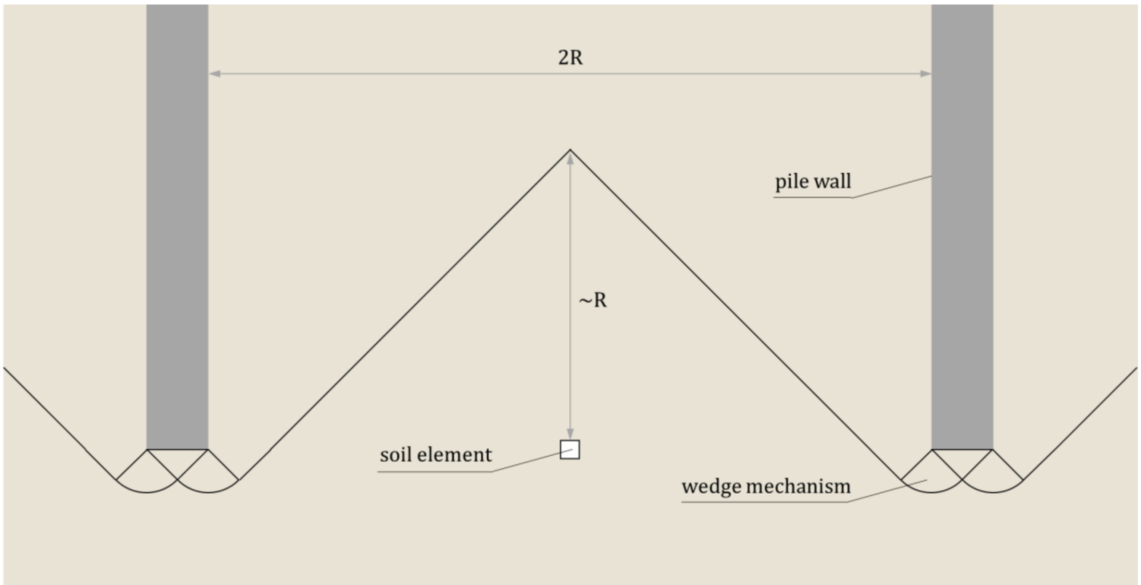

Figure 25: Possible failure mechanism through a vertical cross-section of the pile, to explain the results of case 3-4.

A numerical analysis was carried out using ABAQUS to investigate whether these explanations are reasonable. A simple elastic model with no gravity was used to gain a rough idea of the variation of stresses around the pile base. In reality, soil is a frictional material, and yielding will affect the stresses. Two different models were used, both axisymmetric.

The first model simulated a pile by fixing a pile-shaped section, and applying a stress on the bottom surface and tractions to the inner and outer surfaces. The stresses calculated by this model are shown in *figure 26*. Each load was applied one at a time, so the actual stresses would be a superposition of these results. The stress at the centre of the pile, due to the load applied on the internal surface of the pile shaft, peaks just above the pile base, suggesting that the results from case 3-4 could have been correct if the internal shaft friction term dominated the superposition.

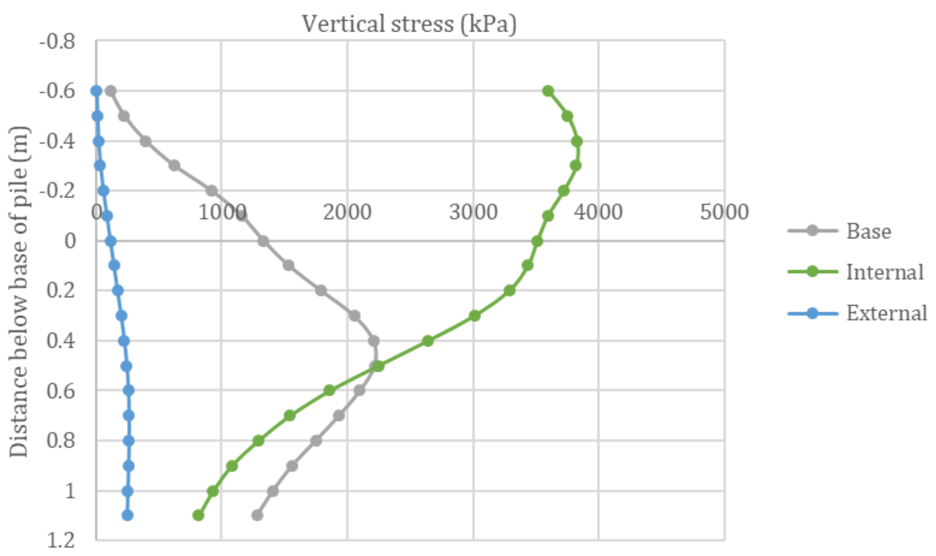

Figure 26: Vertical stresses at the centre of the pile calculated using an elastic ABAQUS model.

The second model used a different material to model the pile, and a vertical force was applied to this pile. This model gave the contours of force shown in *figure 27*. It can be seen that the peak in stress inside the pile is just below the base of the pile. Outside the pile, there is a peak slightly above the base. Note that the grey areas denote zones of tension, which is another considerable simplification made by this model: the soil was modelled as an elastic material which is the same in tension as it is in compression.

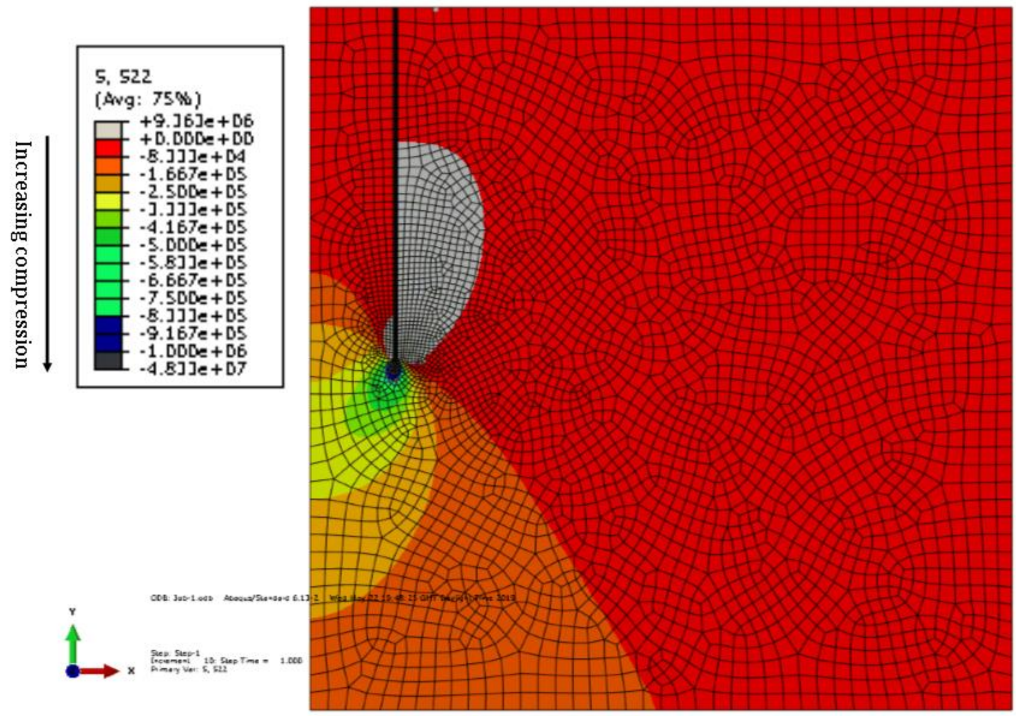

Figure 27: Vertical stress contours around the pile.

3.3.11 Rotation of the internal soil

As explained in section 3.1, rotating the pile relative to the soil column inside should, in theory, prevent the vertical stress from building up in the soil, and therefore prevent plugging. However, if the internal soil begins to rotate with the pile, the benefits of rotating the pile are reduced since there is no relative motion between the internal soil and the pile.

To determine a theoretical installed pile depth at which the internal soil starts to rotate, the torques shown in *figure 28* are equated. This assumes that the entire length of the soil column inside the pile rotates at once, and at the same speed as the pile. Before the soil starts to rotate, there is a torque acting between the soil column and the inside surface of the pile. After the soil starts to rotate, there is a torque acting between the base of the soil column and the surrounding soil. When these two torques are equal, it becomes easier for the internal soil to rotate with the pile than to remain stationary. The derivation is given in *appendix C*, and the resulting theoretical installed pile depth at which the internal soil starts to rotate was found to be between 0.33 m and 0.67 m, depending on the value of the coefficient of lateral earth pressure, K.

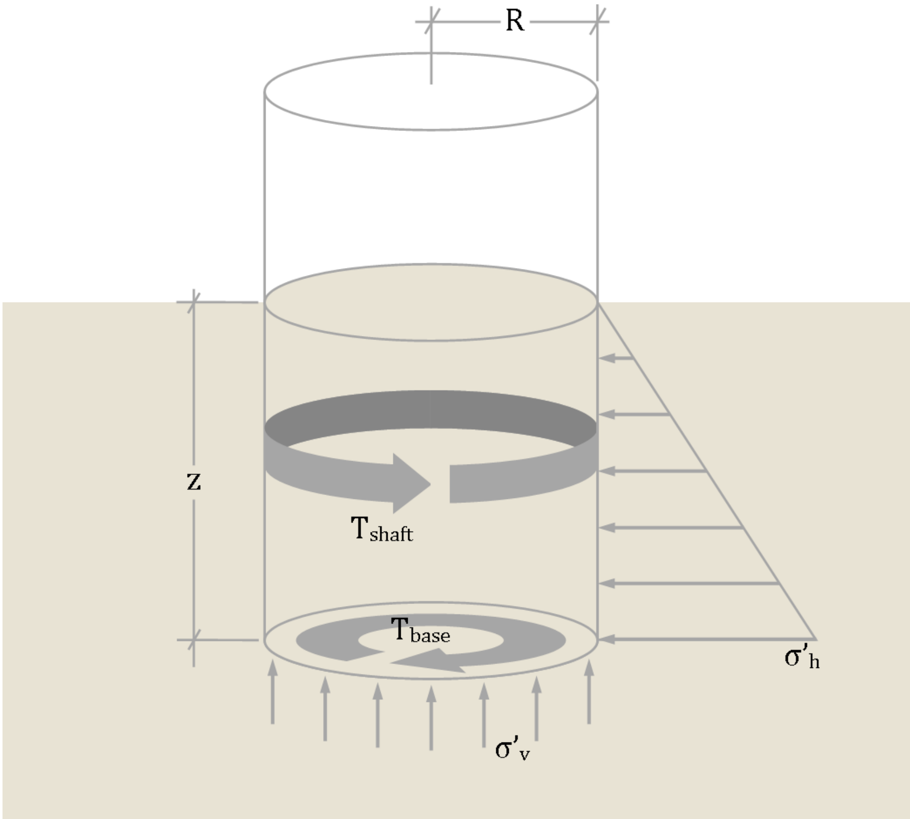

Figure 28: Torques acting on the internal soil before and after it starts to rotate.

As described in section 3.2.3, the elapsed time at the instant the internal soil started to rotate was recorded using a camera, for most of the case 1 tests carried out. The footage only showed when the soil at the surface began to rotate, but the results shown in *table 5* all fit within or very close to the range predicted by the theory, which assumes that the entire column rotates. This suggests that the assumption made in the numerical analysis, that the entire soil column inside the pile rotates as one rigid body, was reasonable.

Table 5: Pile depth at which internal soil starts to rotate.

Case	**Pile depth when soil begins to rotate (m)**
1-4	0.336
1-7	0.523
1-8	0.318
1-9	0.326
1-10	0.317

The resistance that rotary pile driving provides against plugging is therefore lost once an installed depth of about 0.5 pile diameters is reached. If the soil could be prevented from rotating with the pile for as long as possible, it may be possible to retain the benefits of rotary pile driving. To investigate the hypothesis that preventing the rotation of the internal soil will delay the onset of plugging, model tests were carried out and are described in section 4.

4 Secondary Experiments

4.1 Theory and design of experiment

This section describes the tests that were carried out to investigate potential methods of preventing the rotation of the internal soil, and to determine whether this also prevents plugging. The method used involved first installing a thin pile of a different cross-section, then installing a slightly larger tubular pile along the same axis. The thin pile had to be installed deeper than the tubular pile so that it was well anchored and would not rotate. Two different cross-sections of pile were used to compare their effectiveness at preventing the rotation of the soil.

A dimensionless ratio of the approximate maximum available torque and force from the piling machine was used to calculate the appropriate scaled-down maximum torque for corresponding levels of installation force:

$$\frac{T}{FR} = \frac{300\ kNm}{600\ kN \times 0.5\ m} = 1$$

where T and F are the maximum available torque and force provided by the piling machine, respectively, and R is the radius of the pile. During the installation of the tubular pile with a given applied force, the torque was monitored and the installation was ended when either the force or torque limits were reached. The force limit was said to have been reached when the constant applied force was insufficient to install the pile any further.

4.2 Apparatus and experimental techniques

4.2.1 Experiment cases

Case 4: A tubular pile of length 300 mm and cross-section as shown in *figure 29(a)* was pushed into the soil with no pile in the centre, in order to determine the maximum installed depth that could be achieved using various levels of installation force. These results were used as a control, to determine whether preventing the rotation of the soil gave an improvement to the installed depth for a given installation force.

Case 5: A channel, with cross-section as shown in *figure 29(b)*, was used to prevent the rotation of the internal soil. It was placed in the centre of the soil with a horizontal bar attached to its base to simulate a longer pile which is firmly embedded and will not rotate.

Case 6: Similar to case 5, but using a rectangular pile, with cross-section shown in *figure 29(c)*, to prevent the rotation of the internal soil.

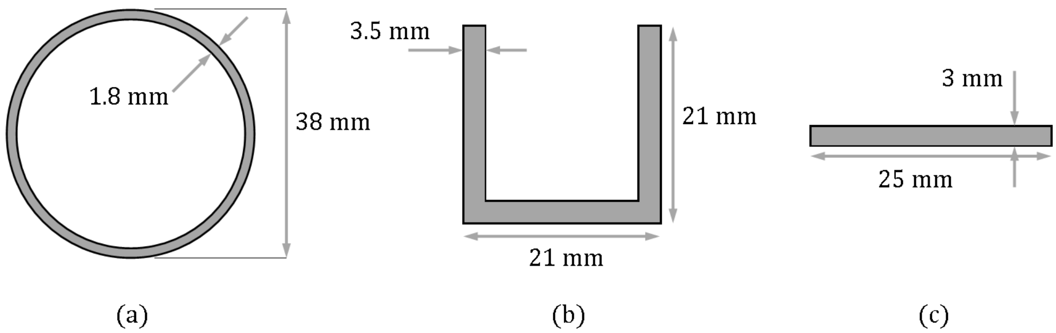

Figure 29: Cross-sections of piles.

4.2.2 Equipment

To measure the torque applied to the pile, a device for measuring torque taken from a vane shear test was connected to the top of the pile, as shown in *figure 30*. The torque shown on the dial of this measurement device was converted into kNm using an upper bound calculation. The failure mechanism assumed a cylinder rotating with the vanes, so the torque could be calculated from the shear strength value given by the vane shear device, given the dimensions of the vanes.

To apply a constant vertical installation force, weights of known values were placed on top of the pile. Weights were gradually applied to the pile at the start of each installation to avoid dynamic effects.

The installed depth of the pile was measured by marking the level of the ground surface on the pile at three points around its circumference. The pile was then extracted, and the distance from the end of the pile to each of the marks was measured using a ruler. These results were checked for consistency and averaged.

Figure 30: Apparatus used for secondary tests (photo: JE Chambers, 2019).

4.2.3 Experimental accuracy

Conversely to the previous experiments, these tests were conducted in the controlled environment of a lab, so the problems that were previously experienced with weather and soil anisotropy do not apply. Here, the main concern is the precision of the equipment. The mechanism of the Giken piling machine ensures that piles are installed exactly vertically, whereas difficulty was experienced in these tests in pushing the pile in straight with nothing to guide it.

To ensure that the results were accurate, at least three repeats were performed for each test. When the three results did not lie within 10 per cent of each other, further repeats were carried out until it was clear which results were anomalous and should be disregarded.

4.3 Results and discussion

4.3.1 Case 4

It was observed that, after a certain depth was reached, rotating the pile did not result in any further penetration, since the force applied by the weights was insufficient to overcome the resistance from the base and shaft at that depth. The available force limits the achievable installation depth, so an increase in applied force results in an increase in installed depth, as shown in *figure 31*.

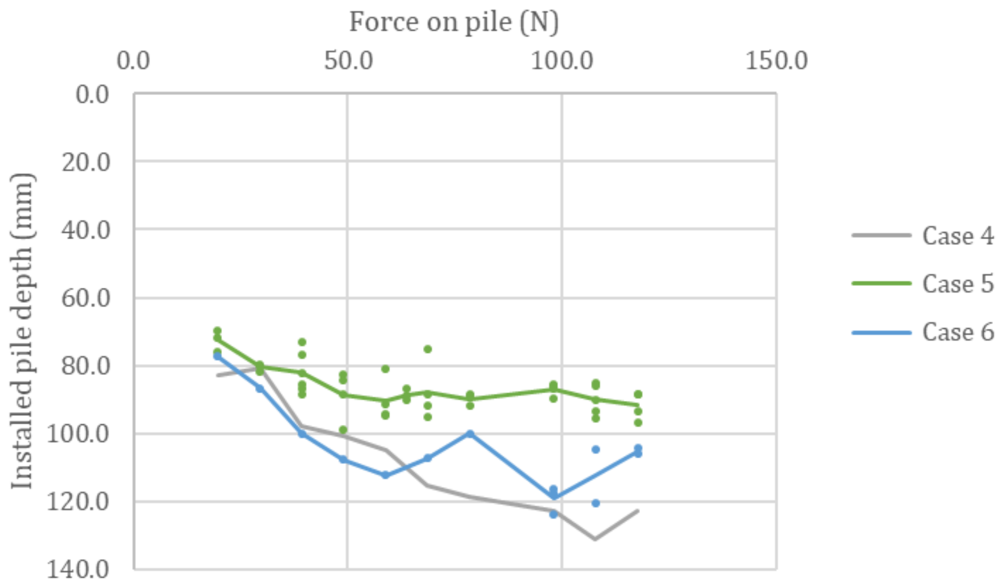

Figure 31: Installed depth against installation force for cases 4, 5 and 6.

Figure 32 shows the maximum torque on the pile for a varying applied force. The torque reaches just under half of that available, so if it were possible to decrease the required force by increasing the required torque, the achievable installed depth would be increased for a given applied force. Cases 5 and 6 attempted to do this.

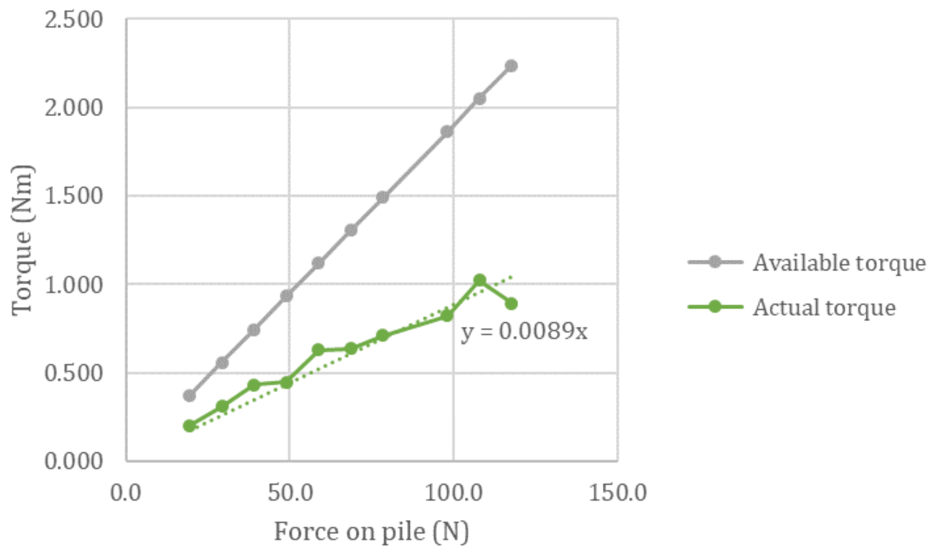

Figure 32: Installation torque against installation force for case 4.

4.3.2 Case 5

Unlike case 4, it was observed that the limiting factor for installation was the available torque, rather than the force. The pile reached the maximum available torque before reaching the depth at which the force had been insufficient to install the pile any further in case 4 (see *figure 31*). This was because the channel was so effective at preventing the rotation of the internal soil. The mechanism of soil rotation was a stationary zone in the centre, surrounded by a slow-moving ring in contact with the wall of the tubular pile.

Considering the theoretical torques due to the shaft friction and the base friction justifies the fact that preventing the rotation of the internal soil quickly leads to much larger torques. When the internal soil is rotating with the pile, the friction between the base of the soil column inside the pile and the surroundings contributes to the torque:

$$T_{base} = \frac{2}{3}\pi\gamma' z R^3 \tan\phi$$

where z is the depth of the pile base into the ground.

When the internal soil is prevented from rotating with the pile, the friction between the internal soil and the inside surface of the pile shaft contributes to the torque:

$$T_{shaft} = \pi\gamma' z^2 R^2 K \tan\delta$$

Therefore, when the internal soil is prevented from rotating with the pile, the torque increases with z^2 rather than z. This means that the torque builds up so fast that the available torque becomes the limiting factor on the achievable installation depth, rather than the available force.

4.3.3 Case 6

Figure 31 on p.39 shows that, as for case 5, the rectangular pile appears to result in a maximum installation depth which is limited by the available torque. However, the limit in this case is reached at a slightly larger installed pile depth than that for case 5. It appears that the rectangular pile is slightly less effective than the channel at preventing the rotation of the internal soil, which means that the torque does not build up so quickly. The mechanism of the rotation of the internal soil observed in case 6 consists of two 'D' shapes rotating separately.

With further investigation, it may be possible to find a shape of pile which optimises the installation process. This pile would prevent just enough rotation so that the torque and force limits are reached at the same time, maximising the installed depth for the existing ratio of torque to force provided by the piling machine.

Alternatively, it may be possible to increase the torque capacity of the piling machine such that pile cross-sections which prevent more rotation of the internal soil can be used, reducing the required installation force even further. A lower bound analysis has been carried out to determine the feasible torque and force that could be applied by the piling machine, given that these are generated from three reaction piles.

To estimate the force that could be provided, the lower bound mechanism shown in *figure 33* was assumed. This mechanism assumes that there are three reaction piles, each providing the same vertical reaction force. Each pile also contributes the same moment, provided by its lateral resistance, to ensure moment equilibrium. The force on pile D was related to the vertical resistance of the other three piles by vertical equilibrium, and the maximum shaft friction that could be provided by each of the reaction piles was calculated using the API method (2000).

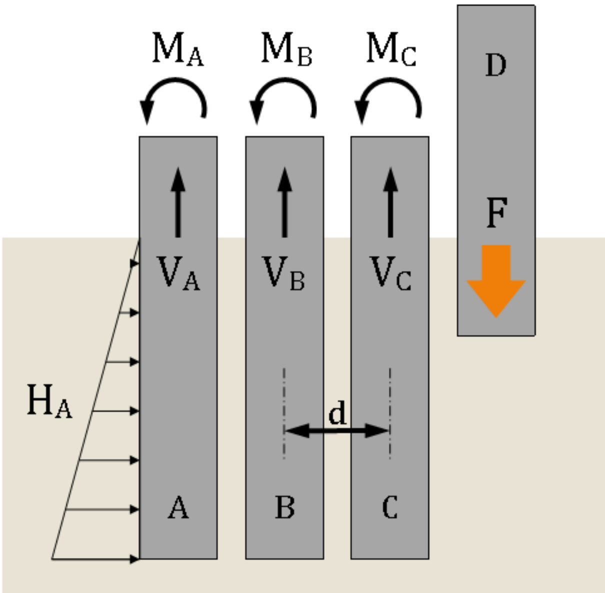

Figure 33: Lower bound mechanism to estimate the maximum force that could be provided by the piling machine.

The full derivation is given in *appendix D*, and resulted in a maximum theoretical force on the pile being installed of:

$$F = 3\pi D L^2 \gamma' K \tan\delta$$

The lower bound mechanism shown in *figure 34* was assumed in order to estimate the maximum torque that could be provided. It assumes that the torque is provided by the lateral resistance of the reaction piles, and that all three piles contribute the same horizontal force to this resistance.

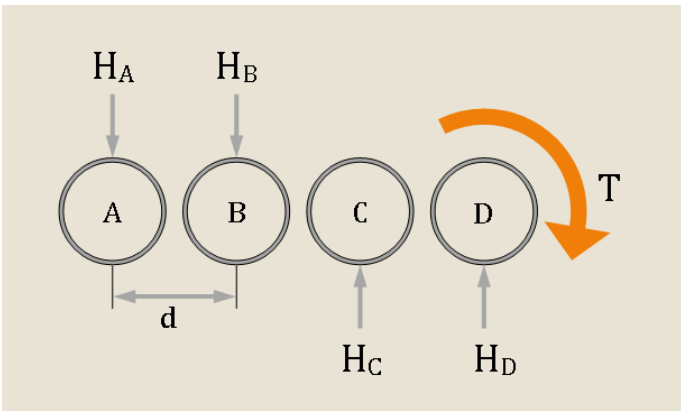

Figure 34: Lower bound mechanism to estimate the maximum torque that could be provided by the piling machine.

The full derivation is given in *appendix E*, and results in a maximum theoretical torque that could be provided by the piling machine of:

$$T = 2K_p^2 dDL^2\gamma'$$

Assuming conservative values for the soil properties, this gives a theoretical torque of 9 000 kNm; a much larger value than the current available torque of about 300 kNm. Therefore, if the piling machine could be modified to apply this increased torque, the proposed method of pre-installing a pile to prevent rotation of the internal soil could be used to increase the achievable installation depth for a given applied force.

The dimensionless ratio of torque and force introduced previously can be calculated using the same assumed values for the geometry and soil properties:

$$\frac{T}{FR} = 12.8$$

5 Conclusions

The shape and position of the pressure bulb caused by plugging during rotary pile driving has been investigated with full-scale field tests, using CPTs to quantify the stress states in the soil. The stress inside the pile decreases over the first 1.5 m, most likely due to the dilatancy of the sand upon shearing. It then increases to a peak at about the level of the pile base. Below the pile base, the stress is largely unaffected. Outside the pile, the stress increases to form a pressure bulb which extends about 1 pile diameter from the centre of the pile, at around the level of the pile base.

The results from case 2 showed that the application of a 400 kN vertical load during the CPTs did not affect the magnitude of the pressure bulb. This is likely to be because the applied load was resisted by the shaft friction rather than the more compliant base response, so the pressure bulb around the base of the pile was not disturbed.

Case 3 investigated the development of the pressure bulb with time, and showed that the stress at the centre of the pile decreased, increased, and then decreased again. It is possible that one of the CPT results was incorrect, since there was no repeat of that test. If it was not an anomalous result, then it suggests a more complicated mechanism within the pressure bulb. Two alternative hypotheses have been presented to justify this result if it was correct.

Using a numerical analysis, the stress inside the pile has been found to increase exponentially with depth, when not rotating with the pile. When the pile is rotated during installation, the relative velocity between the soil and the pile becomes almost horizontal, so the corresponding friction does not contribute to vertical equilibrium. This results in a linear vertical stress distribution through the soil column inside the pile. Therefore, theory suggests that rotary pile driving should not result in plugging.

However, the field testing showed that plugging still occurs during rotary pile driving. This is because the rotation of the internal soil makes the rotation of the pile redundant, since there is no longer any relative motion. The internal soil begins to rotate with the pile once the pile has been installed about 0.5 m, so beyond this point, any benefits derived from rotating the pile are lost.

To attempt to retain the resistance against plugging provided by rotary pile driving beyond the first 0.5 m of installation, it was attempted to prevent the rotation of the internal soil. It was hypothesised that the prior installation of a thin pile along the same axis, longer than the intended depth of installation of the main tubular pile, would provide enough rotational restraint to prevent the rotation of the internal soil.

Model testing was conducted to investigate this hypothesis, and it was discovered that, although this method was effective at preventing the rotation of the internal soil, it did not result in corresponding increases in pile installation depths. This is because the torque due to the friction between the internal soil and the inner surface of the pile shaft increases with depth squared, so the torque quickly builds up when rotation of the soil is prevented.

Only two different shapes of pile cross-section have been investigated here, so it is possible that further experiments could identify an optimum shape of pile cross-section which prevents just enough rotation such that the torque and force limits of the pile-driving machine are reached at the same time.

To delay the onset of plugging during rotary pile driving, either a different technique must be used (such as water injection), or the proposed technique of preventing rotation could be used if the torque capacity of the pile-driving machine was increased. A lower bound analysis showed that it would be possible to increase the torque capacity of the pile-driving machine up to 9 000 kNm, assuming that the lateral resistance is provided by three reaction piles.

Bibliography

1. American Petroleum Institute (API). (2000). *RP2A: Recommended Practice of Planning, Designing and Constructing Fixed Offshore Platforms – Working Stress Design*, 21st edition, Washington. pp.59–61.
2. Carter, M. (1996). Report on water jetting in coarse sand using Giken's GRB piling system. *M.Eng. Thesis*, University of Cambridge.
3. Delano, O. (2010). The application of surging on jacked-in piles. *M.Eng. Thesis*, University of Cambridge.
4. Finlay, T.C.R., White, D.J., Bolton, M.D. and Nagayama, T. (2001). Press-in piling: The installation of instrumented steel tubular piles with and without driving shoes. *5th International Conference on Deep Foundation Practice, Singapore, April*. pp.199–208.
5. GIKEN Ltd. (2018). Private correspondence.
6. GIKEN Ltd. (2018). 'Giken Completes ECO-Park at the OTEPIA Library Complex, Kochi City'. [online] Available at: https://www.giken.com/en/release/giken-completes-eco-park-at-the-otepia-library-complex-kochi-city/ [Accessed 12 May 2019].
7. GIKEN Ltd. (n.d.). 'Press-in Solutions'. [online] Available at: https://www.giken.com/en/press-in_method/press-in_solutions/ [Accessed 12 May 2019].
8. GIKEN Ltd. (n.d.). 'Rotary Press-in'. [online] Available at: https://www.giken.com/en/press-in_method/penetration_tech/rotary_cutting/ [Accessed 12 May 2019].
9. GIKEN Ltd. (2018). [ebook] Kochi: *Gyropress Method*, p.1. Available at: https://www.giken.com/en/wp-content/uploads/press-in_gyropress.pdf [Accessed 12 May 2019].
10. Henke, S. and Grabe, J. (2008). Numerical investigation of soil plugging inside open-ended piles with respect to the installation method. *Acta Geotechnica*, **3**(3), pp.215–223.
11. Ishihara, Y., Haigh, S. and Bolton, M. (2015). Estimating base resistance and N value in rotary press-in. *Soils and Foundations*, **55**(4), pp.788–797.

12. Kikuchi, Y. (2008). Bearing capacity evaluation of long, large-diameter, open-ended piles. *International Conference on Case Histories in Geotechnical Engineering*, *Arlington, Virginia, August*.
13. Ko, J. and Jeong, S. (2015). Plugging effect of open-ended piles in sandy soil. *Canadian Geotechnical Journal*, **52**(5), pp.535–547.
14. Lehane, B. and Gavin, K. (2001). Base resistance of jacked pipe piles in sand. *Journal of Geotechnical and Geoenvironmental Engineering*, **127**(6), pp.473–480.
15. Masood, T. and Mitchell, J. (1993). Estimation of in situ lateral stresses in soils by cone-penetration test. *Journal of Geotechnical Engineering*, **119**(10), pp.1624–1639.
16. Miller, G. and Lutenegger, A. (1997). Influence of pile plugging on skin friction in overconsolidated clay. *Journal of Geotechnical and Geoenvironmental Engineering*, **123**(6), pp.525–533.
17. Murthy, D., Robinson, R. and Rajagopal, K. (2018). Formation of soil plug in open-ended pipe piles in sandy soils. *International Journal of Geotechnical Engineering*. [online] Available at: https://www.tandfonline.com/doi/full/10.1080/19386362.2018.1465742 [Accessed 12 May 2019].
18. Randolph, M., Leong, E. and Houlsby, G. (1991). One-dimensional analysis of soil plugs in pipe piles. *Géotechnique*, **41**(4), pp.587–598.
19. Rockhill D.J., White D.J. and Bolton M.D. (2003). Ground vibrations due to piling operations. *BGA International Conference on Foundations, Dundee, Scotland, September.* pp.743–756.
20. Shepley, P. and Bolton, M. (2014). Using water injection to remove pile base resistance during installation. *Canadian Geotechnical Journal*, **51**(11), pp.1273–1283.
21. Tsinker, G. (1988). Pile jetting. *Journal of Geotechnical Engineering*, **114**(3), pp.326–334.
22. White D. J., Sidhu H.K., Finlay T.C.R, Bolton M.D., Nagayama T. (2000). Press-in piling: The influence of plugging on driveability. *Proceedings of the 8th International Conference of the Deep Foundations Institute, New York, October.* pp.299–310.

Appendices

Appendix A: Derivation of exponential stresses in internal soil

Vertical equilibrium of *figure 4* on page 8:

$$(\sigma_v' + \delta\sigma_v') \times \frac{\pi D^2}{4} = \sigma_v' \times \frac{\pi D^2}{4} + \sigma_v' K \tan\delta \times \pi D \delta z + \gamma' \times \frac{\pi D^2}{4}\delta z$$

$$\left(\frac{\pi D}{4}\right)\delta\sigma_v' = \left(\pi\sigma_v' K \tan\delta + \frac{\pi D \gamma'}{4}\right)\delta z$$

$$\int_0^{\sigma_v'} \frac{D}{4\sigma_v' K \tan\delta + D\gamma'}\, d\sigma_v' = \int_0^h dz$$

let $y = 4\sigma_v' K \tan\delta + D\gamma'$ and $\frac{dy}{d\sigma_v'} = 4K \tan\delta$

$$\frac{D}{4K\tan\delta}\int_{D\gamma'}^{y} \frac{1}{y}\, dy = h$$

$$\frac{D}{4K\tan\delta}\ln\left(\frac{y}{D\gamma'}\right) = h$$

$$\sigma_v' = \frac{D\gamma'}{4K\tan\delta}\left(\exp\left(\frac{4hK\tan\delta}{D}\right) - 1\right)$$

let $\beta = K\tan\delta$ and $\lambda = \frac{4\beta h}{D}$

$$\sigma_v' = \frac{\gamma' h}{\lambda}\left(e^{\lambda} - 1\right)$$

Appendix B: Derivation of stresses in internal soil during rotary pile driving

Vertical equilibrium of *figure 7* on page 12:

$$(\sigma_v' + \delta\sigma_v') \times \frac{\pi D^2}{4} = \sigma_v' \times \frac{\pi D^2}{4} + \gamma' \times \frac{\pi D^2}{4}\delta z$$

$$\delta\sigma_v' = \gamma'\delta z$$

$$\int_0^{\sigma_v} d\sigma_v' = \int_0^z \gamma'\, dz$$

$$\sigma_v' = \gamma' z$$

Appendix C: Derivation of depth at which internal soil starts to rotate

When the soil is stationary, only T_{shaft} (shown in *figure 28* on page 35) acts on the soil, whereas once it has started to rotate, only T_{base} acts on the soil. Therefore, the depth at which the soil starts to rotate can be found by equating the two torques:

$$T_{shaft} = \frac{\sigma_h'}{2}\tan\delta \times R \times 2\pi R z \qquad \textit{where } \sigma_h' = K\gamma' z$$

$$= \pi\gamma' z^2 R^2 K \tan\delta$$

$$T_{base} = \int_0^R \sigma_v' \tan\phi \times r \times 2\pi r\, dr \qquad where\ \sigma_v' = \gamma' z$$

$$= \frac{2}{3}\pi\gamma' z R^3 \tan\phi$$

$$\therefore \frac{2}{3}\pi\gamma' z\, R^3 \tan\phi = \pi\gamma' z^2 R^2 K \tan\delta$$

$$z = \frac{2R\tan\phi}{3K\tan\delta}$$

$$substitute\ in\ R = 0.5m, assume \tan\delta \approx \tan\phi\ , and\ assume\ K = 0.5 \sim 1:$$

$$\therefore z = \frac{1}{3} \sim \frac{2}{3}$$

Appendix D: Derivation of maximum installation force

Assuming $V_A = V_B = V_C$ and $M_A = M_B = M_C = \frac{1}{2}LH_A(L)$, where $H_A(L) = DL\gamma' K_p^2$

Vertical equilibrium of *figure 33* on page 42: $F = 3V_A$

Moment equilibrium of *figure 33* on page 42: $3M_A = 3dV_A + 2dV_B + dV_C = 6dV_A$

$$\therefore F = 3V_A = \frac{3M_A}{2d} = \frac{3LH_A(L)}{4d}$$

Therefore F is the minimum of the two options: $F = \min\left\{3V_A, \frac{3LH_A(L)}{4d}\right\}$

Assuming conservative values for K, δ, ϕ, and d, it can be shown that the available shaft friction limits the value of F, not the lateral resistance, giving:

$$\therefore F = 3\pi DL^2\gamma' K \tan\delta$$

Appendix E: Derivation of maximum installation torque

Assuming $H_A = H_B = H_C$ where $H_A = \frac{1}{2}K_p^2 DL^2\gamma'$

Horizontal equilibrium of *figure 34* on page 42: $H_A + H_B = H_C + H_D$

$$\therefore H_D = H_A$$

Moment equilibrium of *figure 34* on page 42: $T + dH_C = 2dH_B + 3dH_A$

$$\therefore T = 4dH_A = 2K_p^2 dDL^2\gamma'$$

Appendix F: Health and safety review

This project was divided into two parts; the first part was the experiments carried out in Japan, and the second part was the analysis carried out during the academic year in Cambridge.

The health and safety for the first part of this project was managed by Giken. This included an initial health and safety presentation about the typical risks that may be encountered while working at Giken and living in Japan, as well as daily health and safety briefings for the whole team involved in carrying out the experiments. The initial health and safety presentation covered general risks related to working in an office, such as the evacuation routes in case of fire, as well as emergency procedures to be followed in the event of a tsunami. The daily health and safety briefings covered specific risks relating to the tasks that were to be carried out that day. The major risks identified were heat stroke, being struck by objects suspended by the crane, and tripping over the large cables required to power the piling machine. These briefings covered all of the risks that were encountered, and there were no incidents during the test period.

For the second part of the project, a health and safety assessment was carried out based on the foreseeable risks at the beginning of the academic year. The main risks identified were those of fatigue, eye strain, upper limb problems and backache due to overuse or improper use of a computer at a poorly set-up workstation. This assessment was appropriate and covered all of the risks that were encountered. The risks were adequately controlled by ensuring that the workstation was correctly set up.

However, some minor experiments were carried out in the Schofield Centre lab which had not been anticipated at the beginning of the year, and so were not covered by the initial risk assessment. In hindsight, the main risks were low-level risks due to manual handling and working in a lab environment alongside people working on other experiments. There were no incidents during these experiments.

Overall, the risk assessment that was carried out at the start of the year was appropriate given the information that was available at the time, but a second supplementary risk assessment should have been carried out before commencing the tests in the Schofield Centre lab.